

REVIEW ARTICLE

Mapping the cosmological expansion

Eric V Linder

Berkeley Lab & University of California, Berkeley, CA 94720, USA

E-mail: evlinder@lbl.gov

Abstract. The ability to map the cosmological expansion has developed enormously, spurred by the turning point one decade ago of the discovery of cosmic acceleration. The standard model of cosmology has shifted from a matter dominated, standard gravity, decelerating expansion to the present search for the origin of acceleration in the cosmic expansion. We present a wide ranging review of the tools, challenges, and physical interpretations. The tools include direct measures of cosmic scales through Type Ia supernova luminosity distances, and angular distance scales of baryon acoustic oscillation and cosmic microwave background density perturbations, as well as indirect probes such as the effect of cosmic expansion on the growth of matter density fluctuations. Accurate mapping of the expansion requires understanding of systematic uncertainties in both the measurements and the theoretical framework, but the result will give important clues to the nature of the physics behind accelerating expansion and to the fate of the universe.

Contents

1	Introduction	2
1.1	The dynamic universe	3
1.2	Geometry and destiny	4
1.3	Acceleration	7
1.4	Revolution in physics	7
2	Effects of accelerated expansion	8
2.1	Acceleration directly?	8
2.2	Kinematics	9
2.3	Dynamics	11
2.4	True acceleration?	13
2.5	Fate of the universe	15
3	Distance measures	16
3.1	General cosmological distance properties	16
3.2	Type Ia supernovae	20
3.3	Cosmic microwave background	21
3.4	Baryon acoustic oscillations	23

<i>CONTENTS</i>	2
3.5 Other methods	24
3.6 Summary of mapping techniques	25
4 Growth and expansion	26
4.1 Growth of density perturbations	27
4.2 Abundance tests	29
4.3 Gravitational lensing	29
4.4 Testing gravity	30
4.4.1 First steps	30
4.4.2 Problems parametrizing beyond-Einstein gravity	31
4.4.3 Levels of discovery	32
5 Systematics in data and theory	32
5.1 Parameterizing dark energy	33
5.2 Mirage of Lambda	35
5.3 Inhomogeneous data sets	37
5.4 Miscalibrated standard	39
5.5 Malmquist bias	40
5.6 Other issues	40
6 Future prospects	41
6.1 Data and systematics	42
6.2 Mapping resolution	43
6.3 Limits on cosmic doomsday	43
7 Conclusions	44

1. Introduction

A century ago our picture of the cosmos was of a small, young, and static universe. Today we have a far grander and richer universe to inhabit, one that carries information on the strongest and weakest forces in nature, whose history runs from singularities and densities and temperatures far beyond our terrestrial and laboratory access to the vacuum and temperatures near absolute zero. Understanding our universe relies on a wide range of physics fields including thermodynamics, classical and quantum field theory, particle physics, and gravitation.

Perhaps most amazing is that while our universe is huge, it is finite in well defined ways, and can be encompassed and comprehended. The visible universe extends for nearly an equal number of orders of magnitude above the size of the Earth as the proton lies below. The number of particles is of order 10^{80} , large but not unbounded, and the age of the universe is some 14 billion years, only three times the age of the Earth. And the universe is simple in ways we have no right to expect: it is essentially electrically neutral and its large scale dynamics is governed by gravity and no other forces of nature,

it is nearly in thermal equilibrium for most of its history, and the geometry of space is maximally symmetric.

A few characteristics hold where we might be tempted to say, as Alfonso X “The Wise” did in the 13th century: “Had I been present at the creation of the world, I should have recommended something simpler”. The universe has about a billion times more entropy per baryon than expected, and in a related sense has a greatly unequal ratio of matter to antimatter. The dynamics is neither kinetic energy dominated nor potential energy dominated but apparently perfectly balanced, giving the critical energy density and a flat spatial geometry. But the most important cosmological discovery of the 20th century was that the maximal symmetry does not extend to spacetime; that is, we do not live in a steady state universe unchanging in time.

Discovery of the cosmic expansion of space in the 1910s and 1920s and that the evolution arose from a hot, dense, early state called the Big Bang in the 1960s gave rise to modern cosmology as a exemplar of, window on, and laboratory for physics. Ten years ago the discovery of the *acceleration* of that expansion revolutionized cosmology and a great array of overlapping fields of physics. This article addresses our current knowledge of the cosmic expansion and our prospects for exploring it in detail. In particular, we focus on the recent epoch of acceleration and the astrophysical tools for mapping the cosmic expansion history to reveal the nature of new physics beyond our present standard model.

In the remainder of this section we discuss how the expansion of our universe impacts fundamental questions of the origin and fate of the cosmos and everything in it, and its intimate relation with the nature of gravity, as a force itself and reflecting on unification with quantum theory. We present the effects of acceleration in §2, but do not go into the root causes of it, which are highly speculative at this time; see, e.g., the focus issue on dark energy in [1]. Techniques for directly mapping the expansion appear in §3, while §4 briefly mentions indirect effects of acceleration through the growth of structure in the universe. Obtaining an accurate map is crucial to our understanding, and §5 focuses on challenges imposed by systematic uncertainties within the theoretical interpretation and data analysis. For future measurements these may be the key issues in advancing our knowledge. Future prospects for mapping the cosmic expansion from the Big Bang to the final fate are outlined in §6, and §7 summarizes and concludes.

1.1. The dynamic universe

In the 1910s the frequency shift of spectral lines from astronomical sources with respect to laboratory measurements were observed by Slipher and the dynamics of space was found by Einstein within his theory of general relativity. While Einstein, together with de Sitter, acted to counteract the expansion of space and retain a static state through introduction of the cosmological constant, other researchers in the 1920s such as Friedmann and Lemaître calculated the expansion history of a universe containing matter and components with pressure, and Weyl recognized that a physical expansion

scaling linearly with distance occurred naturally. The observations of Hubble in 1929 established the expanding universe as the basis of cosmology.

From the 1930s to 1980s, astronomical observations of the behavior of sources at different redshifts, and the increasing corroboration of redshift as directly related to distance, confirmed the picture of an expanding universe. (For a collection of some important early papers, see [2].) Figure 1 shows the evolution of our capabilities to map the cosmic expansion and the subsequent understanding achieved. Comparison of theoretical calculations and observations with respect to primordial nucleosynthesis and the cosmic microwave background (CMB) radiation clarified the model as one arising from a hot, dense, near singular state given the name Big Bang. However, estimates of the matter density (and even more so other component contributions, save for radiation measured directly in the CMB) remained somewhat vague, and in fact little different from Friedmann's 1922 work. Data could not make a definitive statement as to whether the matter and energy density amounted to less than, equal to, or possibly greater than the critical density needed for a spatially flat, asymptotically static expansion.

This all changed dramatically in 1998 with the discovery of acceleration of the cosmic expansion, by two independent groups mapping the distance-redshift relation of Type Ia supernovae [3, 4]. The expansion history behavior jumped from being somewhere between a critical, matter dominated universe and an open, spatial curvature dominated universe (approaching an empty universe akin to the Minkowski space of merely special relativity), and instead shifted toward one with similarities to de Sitter space governed by a cosmological constant. What was so revolutionary was not that such behavior merely changes the quantitative aspects of the expansion, illustrated in Figure 1, but differs qualitatively and fundamentally, breaking the relation between geometry and destiny.

1.2. Geometry and destiny

For a non-accelerating universe described on large scales by a smooth, homogeneous and isotropic, i.e. Friedmann-Robertson-Walker model, geometry and destiny are inextricably linked. Whether the spatial curvature is positive, zero (flat), or negative correlates one-to-one with whether the expansion is closed (bounded), critical (asymptotically static), or open (unbounded). However, the Einstein field equations governing the cosmic expansion involve not only the amount of energy density but the full energy-momentum contribution. So there is a loophole to escape destiny.

The Friedmann equations (the Einstein equations in a homogeneous, isotropic model) can be written as

$$\dot{a}^2 + k - 8\pi G\rho a^2/3 \equiv \dot{a}^2 + V_{\text{eff}}(a) = 0, \quad (1)$$

where a is the expansion scale factor, k is the spatial curvature, and ρ is the total energy density. Following, e.g., [5], consider the second two terms as making up an effective potential to complement the first, kinetic energy term. From the continuity (or conservation of energy-momentum) equation, the total energy density ρ will evolve with

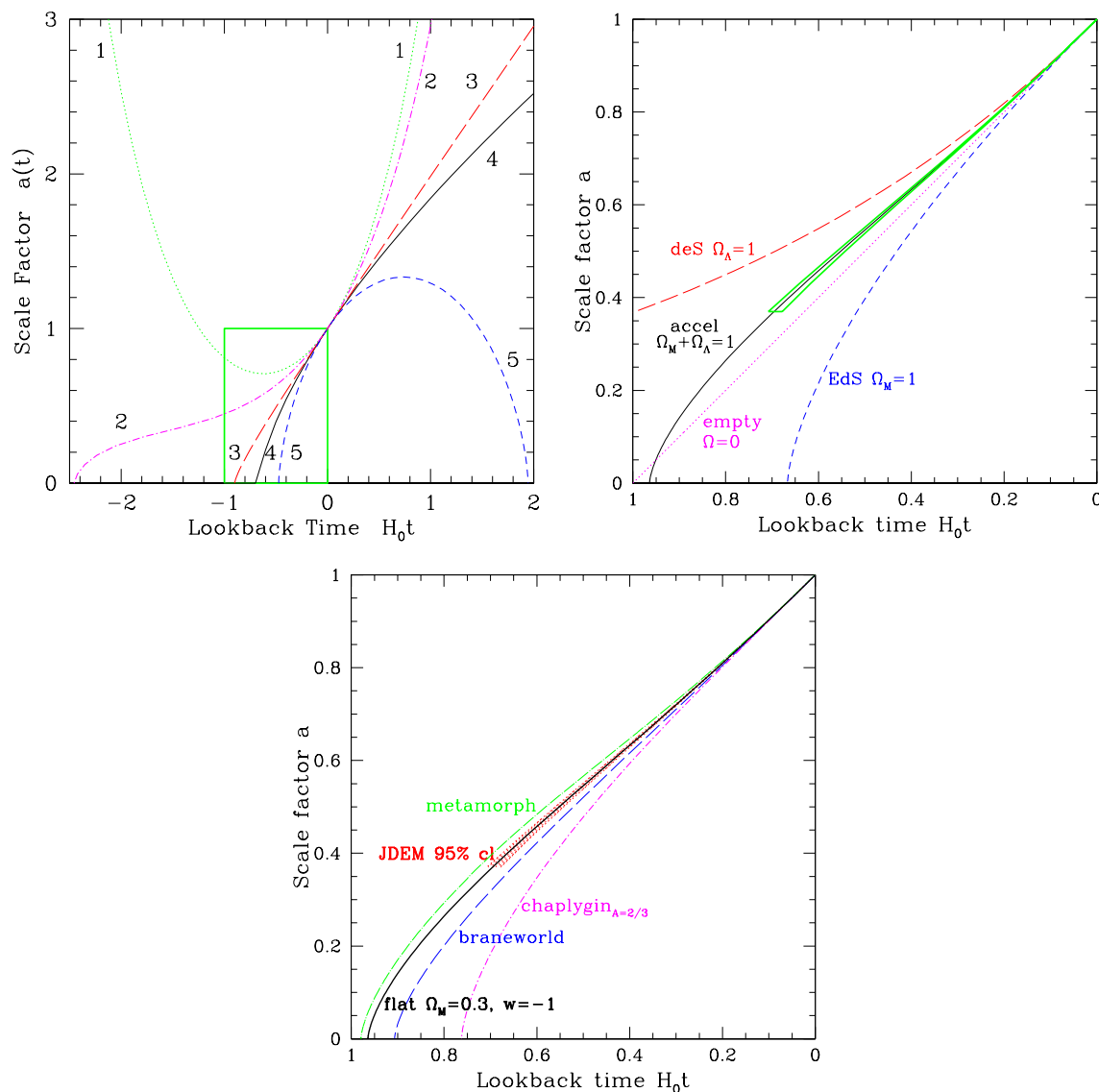


Figure 1. Mapping the expansion history has been a major theme of cosmology, revealing the constituents and nature of our universe. From early models with diverse properties (top left panel), scientists narrowed in to a region shown by the green box corresponding to Big Bang models with a long matter dominated epoch. By the 1980s cosmologists believed the universe corresponded to an Einstein-de Sitter universe with critical matter density, or perhaps some model more toward the empty universe curve (top right panel). The remarkable discovery in 1998 of accelerated expansion showed that the correct model must be similar to the solid black curve, partaking of characteristics of the de Sitter universe with a cosmological constant Λ . The challenge now is to further improve our cosmic mapping ability to zoom in on the narrow green triangular region, revealing the nature of the new physics behind acceleration (bottom panel).

expansion as $\rho \sim a^{-3(1+w)}$, where $w = p/\rho$ is the pressure to energy density, or equation of state, ratio (easily generalized for a time varying ratio). So $\rho a^2 \sim a^{-(1+3w)}$.

If $w > -1/3$ then as seen in Figure 2 the effective potential ranges from $-\infty$ to k for all values of a , i.e. the entire expansion history. Thus, whether the effective potential crosses zero and hence whether there is a maximum value of a or expansion continues without halt is wholly governed by the value of the spatial curvature k : geometry controls density.

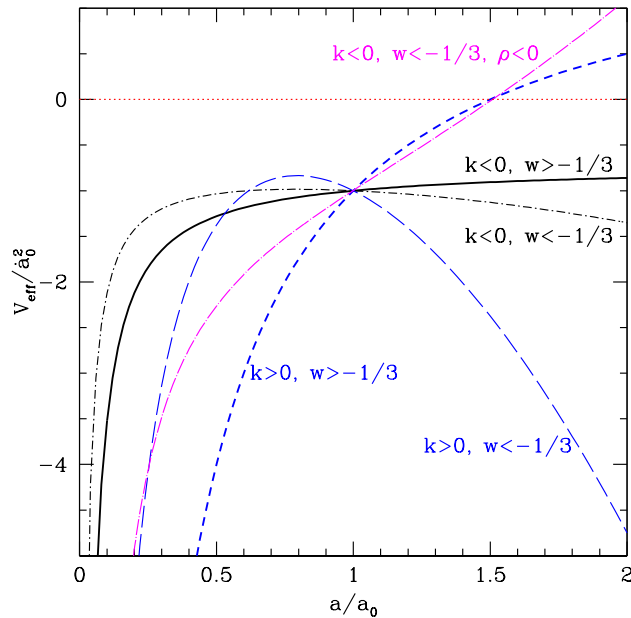


Figure 2. Effective potentials for universes classified according to their geometry (sign of k) and whether the cosmic expansion accelerates ($w < -1/3$) or not. Models crossing the dotted zero line do not expand forever. For $w > -1/3$ the geometry determines the destiny: whether models with physical kinetic energy, hence $V_{\text{eff}} \leq 0$, can achieve $a \rightarrow \infty$, i.e. expand forever. By contrast, for accelerating universes the destiny is eternal expansion regardless of geometry – unless the energy density ρ can go negative.

However, if $w < -1/3$ then the second term of the effective potential eventually dominates as the expansion factor grows large. This strongly negative contribution can overcome a positive k , so one can in fact have an eternal, positive curvature universe. Conversely, if the energy density itself goes negative (e.g. due to a negative cosmological constant) then a finite, negative curvature universe is possible. To determine the crucial quantity, the value of w , we need to take into account the entire energy-momentum not just the energy density. From the other Friedmann equation,

$$\frac{\ddot{a}}{a} = -\frac{4\pi G}{3}(\rho + 3p) = -\frac{4\pi G}{3}\rho(1 + 3w), \quad (2)$$

we see that the condition $w < -1/3$ is precisely the condition for accelerated expansion, $\ddot{a} > 0$. When one of the components of the universe has sufficiently negative pressure and contributes substantial energy density, such so-called dark energy can cause the total equation of state to drop below $-1/3$ and cause acceleration. Destiny then becomes

unhinged from geometry, and we must understand the nature of dark energy to predict the fate of the universe. We discuss this further in §2.5.

1.3. Acceleration

Einstein's equivalence principle states that acceleration is curvature is gravity. While space may (or may not) be flat, *spacetime* curvature is nonzero in an expanding universe. Rather than viewing gravity as a force acting at a distance, we can view it as the curvature of spacetime and particles follow paths of least action (geodesics) in this curved spacetime. An intuitive way of seeing these deep connections is given in Figure 3.

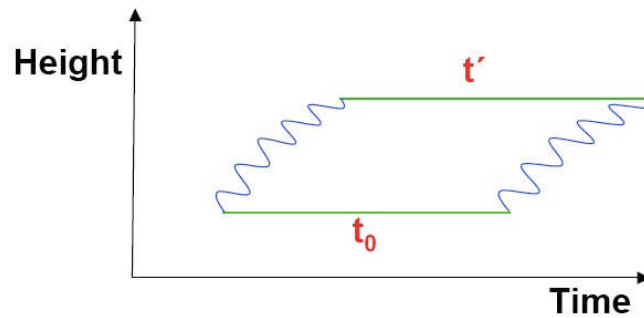


Figure 3. A photon experiences a frequency shift from acceleration, gravity, or spacetime curvature. Here the spacetime diagram illustrates a Pound-Rebka experiment of a photon propagating from one atom to another at height h above it. A gravitational field leads to a gravitational redshift $z = gh/c^2$, while equivalently a uniform acceleration g over a time t leads to a velocity $v = gt$ and a Doppler shift $z = v/c = gt/c = gh/c^2$. Since a frequency change is equivalent to a change of time intervals, the horizontal, parallel line segments representing the emitted photon pulse period t_0 and received period t' cannot be equal. This means the photon propagation lines (wavy diagonal lines), which should each be at 45° in a flat spacetime diagram, must not in fact be parallel. Thus acceleration, gravitation, and spacetime curvature are equivalent.

Thus, mapping the expansion history and its acceleration is equivalent to mapping spacetime or to exploring the gravitational nature of the universe.

1.4. Revolution in physics

Is the discovery and further exploration of cosmic acceleration truly revolutionary? Let us ask what is our current understanding of the universe through the Standard Model: baryons, photons, neutrinos, etc. make up roughly 4% of the energy density of the universe. Understanding 4% is like one letter out of the alphabet, e.g. reading

o o
o o o o o o
 o o o o o
o o o o o o

o o o o o o

 o o o o o o

We may hope to soon detect and eventually characterize dark matter. What will be our understanding once we have succeeded with this characterization and employed it to extend the Standard Model to a new theory of high energy physics such as supersymmetry? Then we will comprehend 25% of the energy density of the universe, like all the vowels (with y) of the alphabet:

e a u e o e y i o e a e e a i u i e e i e e i e y e y
o i e e a i o o y i e a e e o a e o i a o y
e a i e e u e o o e o e u i e e i o e y i e i e o u a i o
o u a u e o y a e a u e o e a u u i i e a o e e o y
o a i a i o a e a u e o a e i e o i y e e e u e o
i e i o e e a i o o a e e y o e e a e o e u i e e

It is apparent that for true understanding we will need to know the nature of dark energy. Only then will we have a complete and comprehensible picture:

The nature of the physics of the accelerating universe is the premier mystery for this generation of physics. The challenge of a new, dominant, strongly negative pressure component of the universe is closely tied with the foundations of quantum theory and the nature of the vacuum; it is central to the theory of gravitation and the nature of spacetime, possibly even the number of dimensions. The behavior of dark energy governs the fate of the universe.

Understanding cosmic acceleration undeniably will extend the frontiers of physics and rewrite the textbooks. It is not excessive to suggest that we are faced with a revolution in our understanding of nature as profound as the mystery of blackbody radiation a century ago. Blackbody radiation taught us the existence of photons and the structure of atoms; dark energy may lead us to the existence of quantum gravity and the structure of the vacuum.

2. Effects of accelerated expansion

2.1. Acceleration directly?

Given the importance of cosmic acceleration, is there some way to detect it in itself, rather than through the curves of the expansion history? Recall Figure 3. There we motivated the Equivalence Principle by showing how acceleration equals gravity. We can detect the acceleration through the cosmological version of the gravitational redshift. Photons (or any signal) will have their frequencies shifted by the acceleration just as they would by a gravitational field. Of course the expansion of space in itself redshifts photons, but that is analogous to a velocity or Doppler shift; acceleration will add a second time derivative of the photon frequency, showing up a drift in the redshift z .

The redshift drift was first discussed by [6] and given in general form by [7]. Analysis of its use as a cosmological probe, including observational challenges and systematics, appeared in [8, 9]. The result is that

$$\dot{z} = H_0(1+z) - H(z) = a^{-1} [H_0 - \dot{a}], \quad (3)$$

where $H = \dot{a}/a$ is the Hubble parameter and H_0 is the present expansion rate, the Hubble constant. Since the scale factor $a = 1/(1+z)$ we clearly see that \dot{z} vanishes only in universes with $\dot{a} = \text{constant}$. That is, redshift drift is a direct signature of acceleration (or deceleration). However, since the Hubble time H^{-1} is more than 10 billion years, the redshift drifts at only 1 part in 10^{10} per year, beyond present technology to measure. Even with a 20 year observational program with stability achieved at the one part in a billion level, the cosmological leverage of such a measurement is unimpressive. Moreover, as [8, 9, 10] pointed out, just as peculiar velocities interfere with accurate redshift measurements, so would peculiar accelerations degrade redshift drift. These can take the form of endpoint effects, i.e. jitter in the observer or source motion due to realistically inhomogeneous gravitational fields from mass flows, or propagation effects such as a stochastic gravitational wave background with energy density as small as 10^{-17} of critical density would generate significant noise.

As for dynamical effects of dark energy within the solar system or astrophysical systems, the energy density is simply too low. All the dark energy within the entire solar system constitutes the energy equivalent of three hours of sunlight at 1 AU, ruling out any direct effect on orbits. For lensing by black holes, say, the relative contribution to the deflection of light by a cosmological constant Λ is $\Lambda r^2/(m/r)$. Detectable lensing requires a gravitational potential $\Phi \sim m/r \gtrsim 10^{-6}$, and $\Lambda \sim H^2$ so it would require a black hole with mass greater than $10^{13} M_\odot$ before dark energy would contribute even 1% effect – and at that point the static approximation used here breaks down. Thus, cosmological expansion remains the practical path to mapping acceleration.

2.2. Kinematics

It is attractive to consider how much information one can extract on the expansion history from minimal assumptions. If one uses only the geometry of spacetime as an input, i.e. the Robertson-Walker metric, then one can learn a remarkable amount. For example, the expansion of space and redshift of photons, hence the decrease in temperature and density as the universe expands, are directly derived from examination of the metric. Such properties that do not rely on supplementing the geometry with equations of motion are referred to as kinematics, while those that depend on the field equations, i.e. the specific theory of gravity, fall under dynamics.

For example, the relation between conformal distance η and the expansion factor a is kinematic,

$$\eta(a_\star) = \int_{a_\star}^1 \frac{da}{a^2 H}, \quad (4)$$

but if H is defined in terms of η , i.e. $H = \dot{a}/a = a^{-2}da/d\eta$, then this becomes a tautology. To actually evaluate the distance-redshift relation requires a model for H , generally supplied by the equations of motion, that is the Friedmann equations in terms of the densities and pressures. Before returning to this, let us consider kinematic signatures of acceleration.

In the diagrams of Figure 1, acceleration would show up as convexity of the curves, i.e. the second derivative becomes positive. A clearer and more direct way of seeing acceleration is by transforming the variables plotted to the conformal horizon scale as a function of expansion factor; see Figure 4. A size of the visible universe can be defined in terms of the Hubble length, H^{-1} , where the expansion, or e-folding, rate $H = \dot{a}/a$. Since all lengths expand with the scale factor a , we can transform into conformal, or comoving, coordinates by dividing by a , thus defining the conformal horizon scale $(aH)^{-1}$.

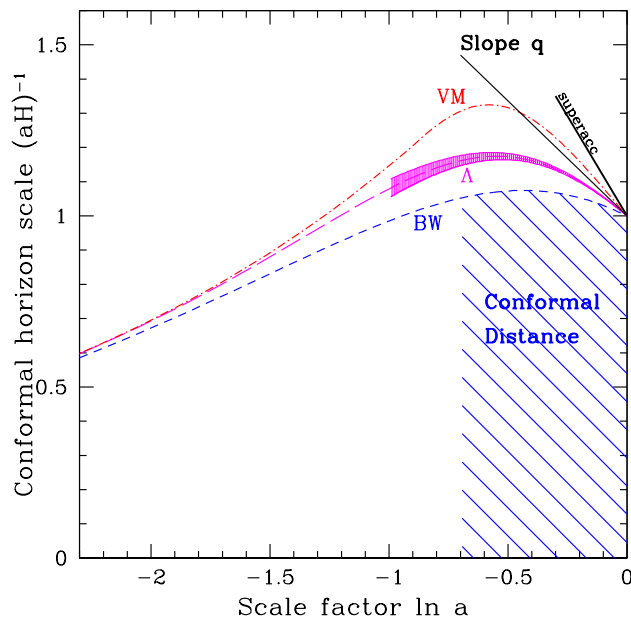


Figure 4. This conformal history diagram presents a unified picture of important properties of the cosmic expansion. Curves represent the expansion history of different cosmological models (here the cosmological constant Λ , an extra dimension braneworld scenario, and a vacuum metamorphosis or quantum phase transition). The value of a point on a curve measures the conformal horizon, basically the size of the universe, as a function of the cosmic expansion factor. The slope of the curve gives the deceleration parameter q ; if it is positive then the universe is decelerating but if the slope is negative the universe is accelerating. The area under a curve gives the distance measured by observers from the present ($a = 1$ or $\ln a = 0$) to some time in the past. The shading around the Λ curve shows how well next generation experiments should probe the cosmic expansion.

Comoving wavelengths would appear as horizontal lines in this plot and so wavelengths enter the horizon, i.e. fall below the horizon history curve, at early times as the universe expands. For decelerating expansion, this is the whole story, with

more wavemodes being revealed as the expansion continues. However, for accelerating universes, the slope of the horizon history curve goes negative and modes can leave the horizon. This is precisely the principle behind inflation as an accelerating epoch in the early universe.

This diagram demonstrates visually the tight connection between the expansion history (the value along the curve), acceleration (the slope of the curve), and distances of objects in the universe (the area under the curve). Thus distances provide a clear and direct method for mapping the expansion history, and will be treated at length in §3.

However, as stated above, to actually evaluate the curve for an expansion history one needs a model for the expansion. One could adopt an ad hoc model $a(t)$ or $H(z)$ or, parameterizing the acceleration directly, $q(z)$ where $q = -a\ddot{a}/\dot{a}^2$ is called the deceleration parameter, or even the third derivative $j = a^2 \ddot{a} / \dot{a}^3$ called the jerk. One runs the danger of substituting the physics of the Einstein equations with some other, implicit dynamics since adopting a form for $q(z)$ is equivalent to some ad hoc equation of motion. Explicitly, if one defines $H^2 = f(\rho)$, some function of the total density, say, then the continuity equation leads to $q = -1 + (3/2)(1 + w) d \ln f / d \ln \rho$, so choosing some functional form $q(z)$, or $j(z)$, is choosing an equation of motion. That is, one has not truly achieved kinematic constraints, only substituted some other unspecified physics for general relativity.

One method for getting around this is by putting no physics into the form by taking a Taylor expansion, e.g. $q(z) = q_0 + q_1 z$ [11, 12]. This has limited validity, that is it can only be applied to mapping the expansion at very low redshifts $z \ll 1$ and it is not clear what has actually been gained. Another method is to allow the data to determine the form, and the physics, through principal component analysis as in [13, 12]. This has a broader range of physical validity, but has substantial sensitivity to noise in the data, since it seeks to extract information on a third derivative in the case of jerk.

2.3. Dynamics

Einstein's equations provide the dynamics in terms of the energy-momentum components in the universe. Note that alterations to the form of the gravitational action also define the dynamics. Unless otherwise specified we consider Friedmann-Robertson-Walker cosmologies. In this case, the simplest ingredients are the energy density and pressure of each component, with the components assumed to be noninteracting. This can be phrased alternately in terms of the present dimensionless energy density $\Omega_w = 8\pi G \rho_w(z=0)/(3H_0^2)$ and the pressure to density, or equation of state, ratio $w = p_w/\rho_w$.

We have seen in §1.2 that the equation of state is central to the relation between geometry and destiny, and it plays a key role in the dynamics of the expansion history as well. In Figure 5 we see the very different behaviors for the dark energy density for different classes of equations of state. The cosmological constant has an unchanging

energy density, and so it defines a unique scale, tiny in comparison to the Planck energy, and a particular time in cosmic history when it is comparable to the matter density. These fine tunings give rise to the cosmological constant problem [14, 15, 16]. Dynamical scalar fields, called quintessence, change their energy density and this may or may not alleviate the large discrepancy with the Planck scale. One of the two main classes of such fields [17], thawing fields that evolve away from early cosmological constant behavior, has energy density that changes little. The other class, freezing fields that evolve toward late time cosmological constant behavior, can have much greater energy density at early times. For example, tracking fields may contribute an appreciable fraction of the energy density over an extended period in the past and may approach the Planck density at early times, while scaling fields mimic the behavior of the dominant energy density component, contributing so much to the dynamics that they can be strongly constrained.

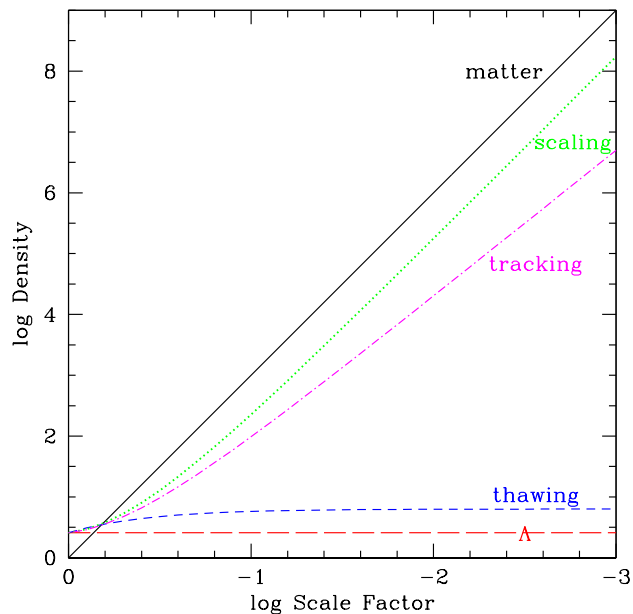


Figure 5. In the recent expansion history, matter and dark energy have contributed similar amounts of energy density (shown here normalized to the present matter density) but this is apparently coincidental. Among quintessence models, the energy density of the cosmological constant or a thawing field differs substantially at early times from freezing fields such as trackers or scalars, one example of classification of dark energy models.

Although there is a diversity of dynamical behaviors [18], these fall into distinct classes of the physics behind acceleration [17]. We see that to reveal the origin of cosmic acceleration we will require precision mapping of the expansion history over the last e-fold of expansion, but we may also need to measure the expansion history at early times. And to predict the future expansion history and the fate of the universe requires truly understanding the nature of the new physics – for example knowing whether dark energy will eventually fade away, restoring the link between geometry and destiny.

2.4. True acceleration?

Before proceeding further we can ask whether the Robertson-Walker model of a homogeneous, isotropic universe is indeed the proper framework for analyzing the expansion history. Certainly the global dynamics of the expansion follows that of a Friedmann-Robertson-Walker model (FRW), as the successes of Big Bang nucleosynthesis, cosmic microwave background radiation measurements, source counts etc. show [19, 20], but one could imagine smaller scale inhomogeneities affecting the light propagation by which we measure the expansion history. This has long been known [21, 22, 23] and for stochastic inhomogeneities shown to be unimportant in the slow motion, weak field limit [24].

To grasp this intuitively, consider that the expansion rate of space is not a single number but a 3×3 matrix over the spatial coordinates. The analog of the Hubble parameter is (one third) the trace of this matrix, so inhomogeneities capable of altering the global expansion so as to mimic acceleration generically lead to changes in the other matrix components. This induces shear or rotation of the same order as the change in expansion, leading to an appreciably anisotropic universe. Observations however limit shear and rotation of the expansion to be less than 5×10^{-5} – 10^{-6} times the Hubble term [25].

Thus, to create the illusion of acceleration one would have to carefully arrange the material contents of the universe, adjusting the density along the line of sight (spherical symmetry is not wholly necessary with current data quality). Again, this has long been discussed [26, 27, 28] and indeed changes the distance-redshift relation. The simple model of [29] poses the problem in its most basic terms, clearly demonstrating its meaning. It considers an inhomogeneous, matter only universe with a void ($\alpha = 0$ for the Dyer-Roeder smoothness parameter) somewhere along the line of sight, extending from z_1 to $z_1 + \Delta z$, and finds that the distances to sources lying at higher redshift do not agree with the FRW relation. Even for very high redshift sources where the cosmic volume is essentially wholly described by FRW there maintains an asymptotic fractional distance deviation of $\Delta z / (1 + z_1)$ (if the void surrounds the observer then the deviation is of order Δz^2).

Suppose we were to define $w(z)$ in terms of derivatives of distance with respect to redshift. Then we would find for certain choices of void size and location that $w(z) < -1/3$; see Figure 6. Apart from the fact that this would require enormous voids, it would be a mistake to interpret this as apparent acceleration within this very basic, matter only model. The analysis is physically inconsistent because it treats the expansion, e.g. $H(z)$, in two different ways: as dynamics, for example in the friction term in the Raychaudhuri or beam equation, and as kinematics, through the correspondence to the differential of the distance, $dr/dz \sim H$. We emphasize this point: in models with inhomogeneities, it is inconsistent to treat dynamics and kinematics the same. See [30] for further discussion of the proper physical interpretation of acceleration.

While the previous approach can deliver a mirage of, but not physical, acceleration,

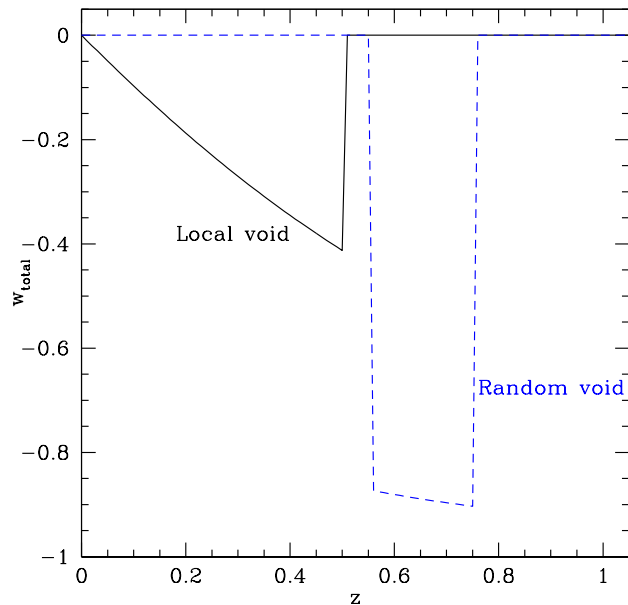


Figure 6. Huge voids can give the illusion of an effective negative equation of state and acceleration, but not the dynamical reality. The solid curve gives the effective total equation of state if we observe from the center of a void extending out to $z = 0.5$, yet interpret data within a smooth FRW model. The dashed curve corresponds to a void in a shell from $z = 0.55 - 0.75$.

one cannot even obtain such an illusion if one requires other basic aspects of FRW to hold. From the Raychaudhuri beam equation in FRW generalized to arbitrary components and smoothness [31], one finds the following two conditions,

$$\Omega_m(z) = 1 + 3w_{\text{tot}}(z) \quad ; \quad \alpha(z) = \frac{1 + w_{\text{tot}}}{1 + 3w_{\text{tot}}} , \quad (5)$$

must hold for a pure matter, inhomogeneous model to mimic a smooth model with matter plus an extra component with equation of state w (so the total equation of state is w_{tot}). These follow from matching the Raychaudhuri equation term by term between the models, so that the distance-redshift relations will agree. However, the requirement of positive energy density then immediately demonstrates that an effective $w_{\text{tot}} < -1/3$ cannot be attained, i.e. acceleration is not possible. Moreover, the matter in the inhomogeneous dust model cannot consistently obey the usual continuity equation.

Thus, a pure dust model with inhomogeneities described by spatial under- and overdensities, i.e. $\alpha(z)$, cannot give distances matching an accelerating FRW universe distance-redshift relation, nor any FRW model without introducing nonstandard couplings in the matter sector.

Finally, to obtain even the mirage of a perfectly isotropic distance-redshift relation requires the inhomogeneities to be arranged in a spherically symmetric manner around the observer, raising issues of our preferred location. If the inhomogeneities are arranged only stochastically, i.e. do not have an infinite coherence length caused by special

placement, then the effects along the line of sight will average out and the distance-redshift relation will reflect the true global expansion. Thus, save for hand fashioning a universe to deceive, observed acceleration is real acceleration.

2.5. Fate of the universe

Given accelerated expansion at present, we still cannot absolutely predict the future expansion and the fate of the universe. If the acceleration from dark energy continues then the universe becomes a truly dark, cold, empty place. The light horizon, within which we can receive signals, grows linearly with time, as always, but the particle horizon giving the (at some time) causally influenced region grows more quickly in an accelerating universe (exponentially in the cosmological constant case). Thus, though formally our observational reach out into the universe increases, we see an ever tinier fraction of the causal universe. (See [32] for more on horizons.)

Also, although the light horizon expands, in a real sense the visible universe does “close in” around us not through objects going beyond the horizon but through their fading away to our sight. For example, in a cosmological constant dominated universe the redshift of an object at constant comoving distance increases exponentially with time, so its received flux decreases exponentially and its surface brightness fades exponentially from the usual $(1+z)^4$ law. Conversely, the comoving distance to a fixed redshift decreases exponentially with time, so vanishingly few objects lie within the volume to any finite redshift and hence have non-infinitesimal flux and surface brightness. (See [33, 34, 5] for some specific calculations.) Thus our view of the universe does not so much shrink as darken. (So dark energy is well named.)

The existence of a Rindler horizon arising from acceleration [35] brings another set of physics puzzles, best known for the borderline case of $w = -1$. In de Sitter space the horizon causes loss of unitarity and makes it problematic to define particle interaction probabilities through an S matrix [14]. On the other hand, the horizon may be instrumental in obviating the Big Rip fate. For a universe with $w < -1$ the increasing (conformal) acceleration overcomes all other binding forces, ripping planets, atoms, etc. apart [36]. However, Unruh radiation, or thermal particle creation from the horizon, with temperature $T \sim g$ and hence energy density $\rho \sim T^4$ where $g = \ddot{a}/a$ is the conformal acceleration (so the rip condition is not $\ddot{a} > 0$ but $(\ddot{a}/a)' > 0$), should quickly overwhelm the dark energy (whose density increases as g , not g^4). Thus the horizon should act to either decelerate the universe or bring the expansion to some non-superaccelerating state [37].

Other possibilities for the fate of the universe include collapse ($a \rightarrow 0$) if the dark energy attains negative values of its potential, as in the linear potential model [38] (also see §6.3), collapse and bounce into new expansion as in the cyclic model [39], or eternal but decelerating expansion if the dark energy fades away.

Thus we have seen throughout this section that to distinguish the origin of cosmic acceleration we may need not only to map accurately the *recent* expansion history, but

distinguish models of dark energy through their *early* time behavior and understand their nature well enough to predict their *future* evolution. To truly understand our universe we must map the cosmic expansion from $a = 0$ to $a = \infty$ – and possibly back to $a = 0$ again.

3. Distance measures

Distance measurements as a function of scale factor or redshift directly map the expansion history. Here we consider several approaches to these measurements, starting with the geometric or mostly geometric methods that give the cleanest probes of the expansion. Many other techniques involving distances exist, also containing noncosmological quantities. One can categorize probes into ones depending (almost) exclusively on geometry, ones requiring some knowledge of the mass of objects to separate out the distance dependence, and ones requiring not only knowledge of mass but the thermodynamic or hydrodynamical state of the material, i.e. mass+gas probes. The discussion here focuses on the geometric distance techniques actually implemented to date, though we do briefly mention some other approaches.

3.1. General cosmological distance properties

Because distances are integrals over the expansion history, which in turn involves an integral over the equation of state, degeneracies exist between cosmological parameters contributing to the distance. These are common to all distance measurements. Figures 7-8 illustrate the sensitivity and degeneracy of various expansion history measurements to the cosmological parameters. Here d is the luminosity or angular distance (we consider fractional precisions so the distinguishing factor of $(1+z)^2$ cancels out), H is the Hubble parameter, or expansion rate, and the quantities $\tilde{d} = d(\Omega_m h^2)^{1/2}$, $\tilde{H} = H/(\Omega_m h^2)^{1/2}$, where h is the dimensionless Hubble constant, are relative to high redshift.

First we note that for a given fractional measurement precision, distances contain about as much information as the Hubble parameter, despite the extra integral (the greater lever arm acts to compensate for the integral). That is (assuming flatness for simplicity),

$$d = \int dz/H, \quad (6)$$

$$\frac{1}{d} \frac{\partial d}{\partial \theta} = - \int \frac{dz}{H^2} \frac{\partial H}{\partial \theta} \bigg/ \int \frac{dz}{H} = - \left\langle \frac{\partial \ln H}{\partial \theta} \right\rangle, \quad (7)$$

for a parameter θ , where angle brackets denote the weighted average. However, surveys to measure distances to a given precision can be much less time consuming than those to measure the Hubble parameter.

Concerning the physical interpretation of the Fisher sensitivities, recall that

$$\delta\theta = \delta(\ln d) \bigg/ \left(\frac{\partial \ln d}{\partial \theta} \right). \quad (8)$$

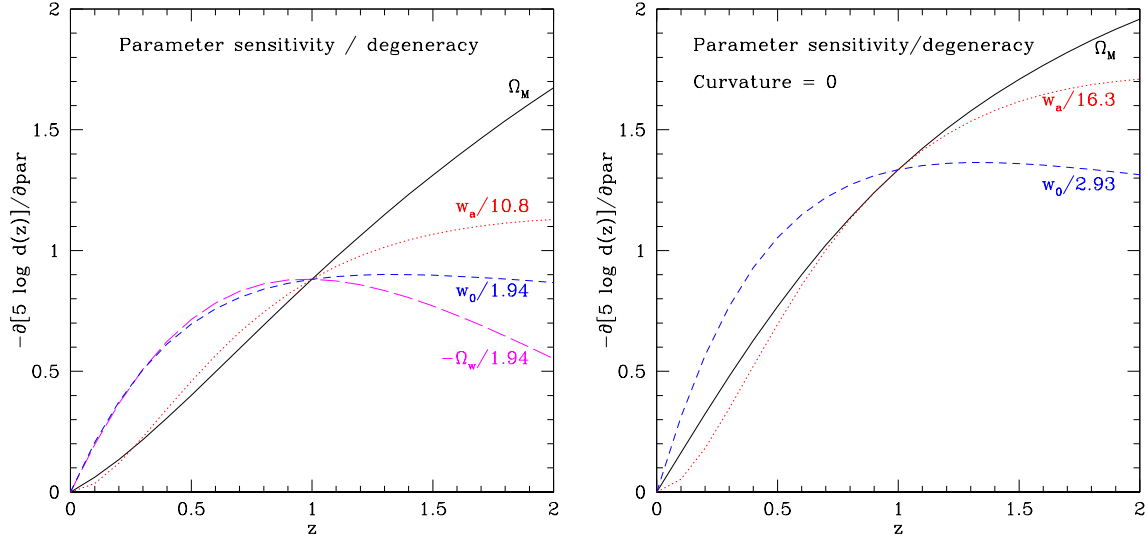


Figure 7. Fisher sensitivities for the magnitude ($5 \log d$) are plotted vs. redshift for the case leaving spatial curvature free (left panel) and fixing it to zero, i.e. a flat universe (right panel). Since only the shapes of the curves matter for degeneracy, parameters are normalized to make this more evident. Observations out to $z \geq 1.5$ are required to break the degeneracies.

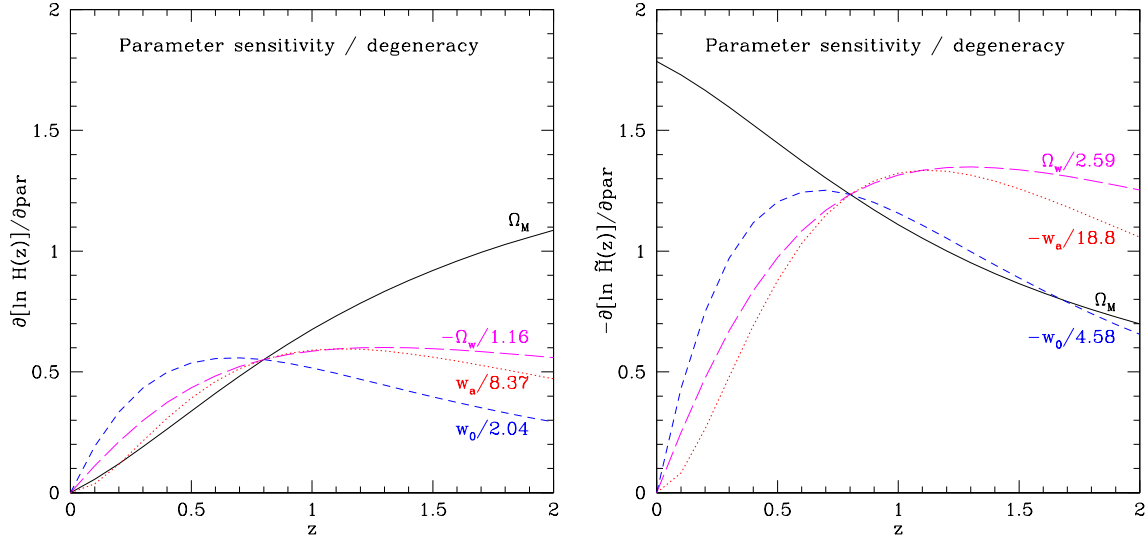


Figure 8. Fisher sensitivities for the Hubble parameter H (left panel) and reduced Hubble parameter $\tilde{H} = H/(\Omega_m h^2)^{1/2}$, i.e. Hubble parameter relative to high redshift (right panel), are plotted vs. redshift, leaving spatial curvature free. The behavior is similar to that in Figure 7 but the degeneracies are somewhat more severe.

If for some parameter the Fisher partial derivative at some redshift is 0.88, say, then a 1% measurement gives an unmarginalized uncertainty on the parameter of 0.011. If

the parameter is $w_a/10.8$, say, this means the unmarginalized uncertainty on w_a is 0.12. The higher the denominator in the parameter label, the less sensitivity exists to that parameter.

The greatest sensitivity is to the energy densities in matter and dark energy; note that we do not here assume a flat universe. The nature of the dark energy is here described through the equation of state parametrization $w(a) = w_0 + w_a(1 - a)$, where w_0 is the present value and w_a provides a measure of its time variation. This has been shown to be an excellent approximation to a wide variety of origins for the acceleration [40]. Sensitivity to w_a is quite modest so highly accurate measurements are required to discover the physics behind acceleration.

Note that degeneracies between parameters, e.g. Ω_m and w_a , and Ω_w and w_0 , are strong at redshifts $z \lesssim 1$. Not until $z > 1.5$ do distance measurements make an appreciable distinction between these variables. This determines the need for mapping the expansion history over approximately the last e-fold of expansion, i.e. to $a = 1/e$ or $z = 1.7$. Since the flux of distant sources gets redshifted, this requires many observations to move into the near infrared, which can only be achieved to great accuracy from space.

From the right panel of Figure 7 we see that the degeneracy between the matter density Ω_m and dark energy equation of state time variation w_a holds regardless of whether space is assumed flat or not. The dark energy density Ω_w and the dark energy present equation of state w_0 stay highly degenerate in the curvature free case, whether considering d or \tilde{d} (not shown in the figure).

From the relation between the derivatives of the distance with respect to cosmological parameters, as a function of redshift, one can intuit the orientation of confidence contours in various planes. For example, the sensitivity for the matter density and dark energy density enter with opposite signs, so increasing one can be compensated by increasing the other, explaining the low densities to high densities diagonal orientation in the Ω_m - Ω_Λ plane. Since the sensitivity to Ω_m trends monotonically with redshift, while that of Ω_w has a different shape, this implies that observations over a range of redshifts will rotate the confidence contours, breaking the degeneracies and tightening the constraints beyond the mere power of added statistics. Similarly one can see that contours in the Ω_m - w_0 plane will have negative slope, as will those in the w_0 - w_a plane.

For the tilde variable \tilde{d} , that is distances relative to high redshift rather than low redshift, there is relatively little degeneracy between the matter density and the other variables – but there is also much less sensitivity to the other variables. The equivalent normalized variables to those in the top left panel of Figure 7 are $\Omega_w/6.60$, $-w_0/6.59$, and $-w_a/36.7$. This insensitivity is why contours in the Ω_m - Ω_w or Ω_m - w planes are rather vertical for distances tied to high redshift, like baryon acoustic oscillations. Of course since the degeneracy directions between distances tied to low redshift and those tied to high redshift are different, these measurements are complementary. (Although not as much in the w_0 - w_a plane, since high redshift is essentially blind to these parameters so tilde and regular distances have the same dependence.)

For the Hubble parameter, a nearly triple degeneracy exists between Ω_m , Ω_w and w_a out to $z \approx 1$. Interestingly, for \tilde{H} there is a strong degeneracy between Ω_m and w_0 for $z \approx 1 - 2$, while the Ω_w - w_a degeneracy remains. It is quite difficult to observe $H(z)$ directly, i.e. measured relative to low redshift; more common is measurement relative to high redshift as through baryon acoustic oscillation in the line of sight direction (see §3.4). Here, the sensitivity to the dark energy equation of state is reduced relative to the distance case, even apart from the degeneracies (since \tilde{H} does not include the $z \lesssim 1$ lever arm).

For either \tilde{d} or \tilde{H} the correlation between energy densities is reversed from the regular quantities, so the likelihood contour orientation in the Ω_m - Ω_Λ plane is reversed as well, close to that of the CMB, another measurement tied to the high redshift universe. The contour in Ω_m - w_0 is similarly reversed but not in w_0 - w_a . Thus, all these varieties of distance measurements have similar equation of state dependencies and, unfortunately, no substantial orthogonality can be achieved in this plane.

To emphasize this last point, Figure 9 illustrates the degeneracy directions for contours of constant Hubble parameter and constant matter density at various redshifts. As we consider redshifts running from $z = 0$ to $z \gg 1$, the isocontours only rotate moderately. Since they always remain oriented in the same quadrant, orthogonality is not possible.

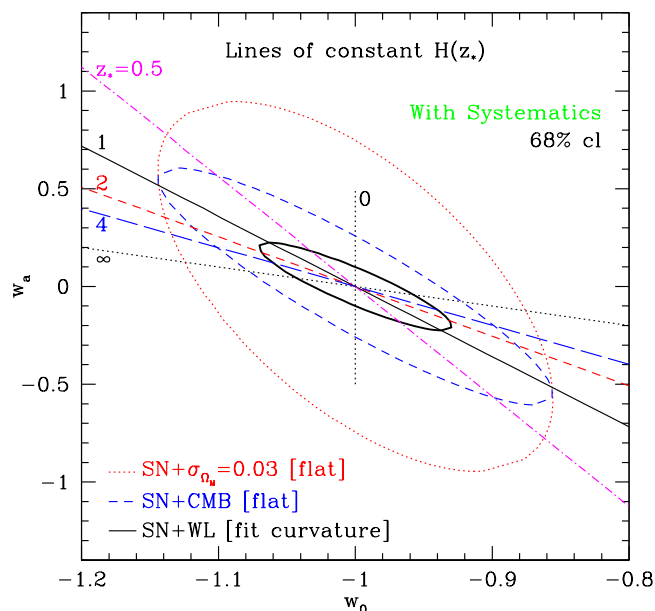


Figure 9. Lines of constant expansion history, i.e. Hubble parameter, are plotted in the dark energy equation of state plane. Observations over a range of redshifts give complementarity, but never complete orthogonality. Contours show approximate examples of how certain combinations of distance probes effectively map different parts of the expansion history.

Conversely, while not giving as much complementarity in the dark energy equation

of state as we might like, the use of different probes can be viewed as giving complementarity in mapping the expansion history. Observations of distances out to $z = 1.7$, e.g. through supernova data, plus weak lensing are basically equivalent to mapping the expansion at $z \approx 1.5$, supernovae plus CMB give it at $z \approx 0.8$, while supernovae plus a present matter density prior provide it at $z \approx 0.3$.

In this subsection we have seen that a considerable part of the optimal approach for mapping the expansion history is set purely by the innate cosmological dependence, and the survey design must follow these foundations as basic science requirements. The purpose of detailed design of successful surveys is rather to work within this framework to minimize systematic uncertainties in the measurements, discussed in more detail in §5. These two requirements give some of the main conclusions of this review.

3.2. Type Ia supernovae

The class of exploding stars called Type Ia supernovae (SN) become as bright as a galaxy and can be seen to great distances. Moreover, while having a modest intrinsic scatter in luminosity, they can be further calibrated to serve as standardized candles. Used in this way as distance measures, studies of SN led to the discovery of the acceleration of the universe [3, 4].

As of the beginning of 2008, over 300 SN with measurement quality suitable for cosmological constraints had been published, representing the efforts of several survey groups. Finding a SN is merely the first step: the time series of flux (the lightcurve), must be measured with high signal to noise from before peak flux (maximum light) to a month or more afterward. This must be done for multiple wavelength bands to permit dust and intrinsic color corrections. Additionally, spectroscopy to provide an accurate redshift and confirmation that it is a Type Ia supernova must be obtained. See [41] for further observational issues. (Also see [42] for the use of Type II-P supernovae.)

Once the multiwavelength fits and corrections are carried out, one derives the distance, often spoken of in terms of the equivalent magnitude or logarithmic flux known as the distance modulus. The distance-redshift or magnitude-redshift relation is referred to as the Hubble diagram. This, or any other derived distance relation, can then be compared to cosmological models.

Analysis of the world SN data sets published as of the start of 2008, comprising 307 SN, show the expansion history is consistent with a cosmological constant plus matter universe, Λ CDM, but also with a great variety of other models [43]. Essentially no constraints on dark energy can be placed at $z > 1$ and the limits on time variation are no more stringent than the characteristic time scale being of the Hubble time or shorter. Figure 10 shows that even for a flat universe and constant equation of state there is considerable latitude in dark energy characteristics and that systematic uncertainties need to be reduced for further numbers of SN to be useful.

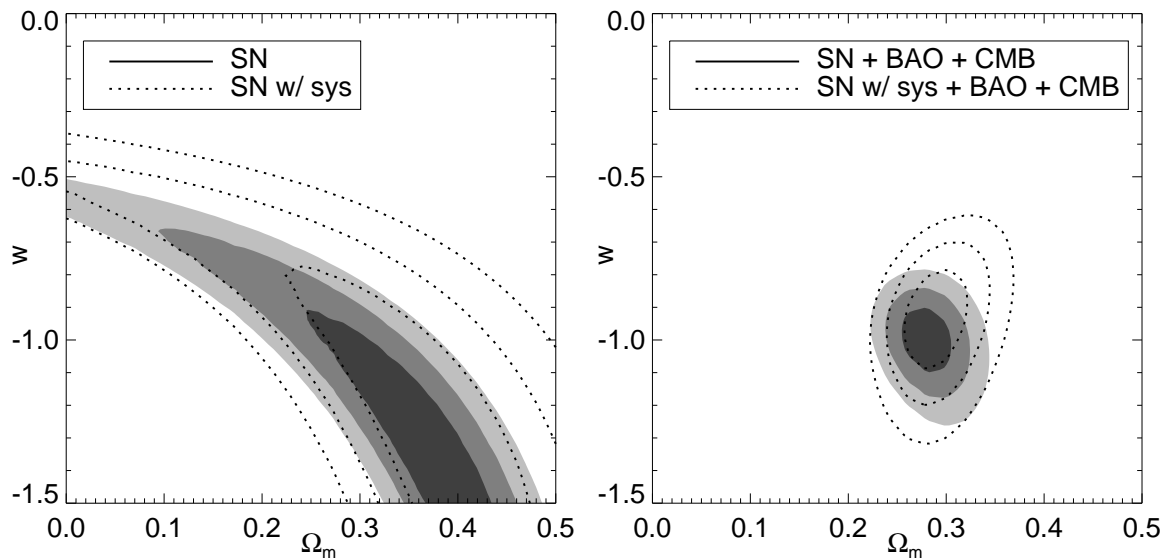


Figure 10. 68.3%, 95.4%, and 99.7% confidence level contours on the matter density and constant equation of state from the Union 2007 set of supernova distances. The left panel shows SN only and the right panel includes current CMB and baryon acoustic oscillation constraints. From [43].

3.3. Cosmic microwave background

The geometric distance information within the cosmic microwave background radiation (CMB) arises from the angular scale of the acoustic peaks in the temperature power spectrum, reflecting the sound horizon of perturbations in the tightly coupled photon-baryon fluid at the time of recombination. If one can predict from atomic physics the sound horizon scale then it can be used as a standard ruler, with the angular scale then measuring the ratio of the sound horizon s to the distance to CMB last scattering at $z_{\text{ls}} \approx 1089$. Related, but not identical to the inverse of this distance ratio, $R = \sqrt{\Omega_m h^2} d_{\text{ls}}$ is often called the reduced distance or CMB shift parameter. This gives a good approximation to the full CMB leverage on the cosmic expansion for models near Λ CDM [44]; for nonstandard models where the sound horizon is affected, this needs to be corrected [43] or supplemented [45].

Because the CMB delivers a single distance, it cannot effectively break degeneracies between cosmological parameters on its own. While some leverage comes from other aspects than the geometric shift factor, the dark energy constraints tend to be weak. However, as a high redshift distance indicator the CMB does provide a long lever arm useful for combination with other distance probes (effectively the $z = \infty$ line in Figure 9), and can strongly aid in breaking degeneracies [46].

The reduced distance to last scattering, being measured with excellent precision – 1.8% in the case of current data and the possibility of 0.4% precision with Planck data – defines a narrow hypersurface in cosmological parameter space (see, e.g., [47]). From Figure 11 we see that the acoustic peak structure contains substantial geometric

information for mapping the cosmological expansion. This will provide most of the information on dark energy since cosmic variance prevents the low multipoles from providing substantial leverage (and almost none at all to the geometric quantities, as shown by the similarity of dashed and solid contours). Polarization information from E -modes and the cross spectrum improves the geometric knowledge. The distance ratio d_{ls}/s of the distance to last scattering relative to the sound horizon is determined much better (almost 20 times so) than the reduced distance to last scattering $R = \sqrt{\Omega_m h^2} d_{\text{ls}}$, but there is substantial covariance between these quantities (as evident in the right panel) for models near Λ CDM (unless broken through external priors on, e.g., the Hubble constant).

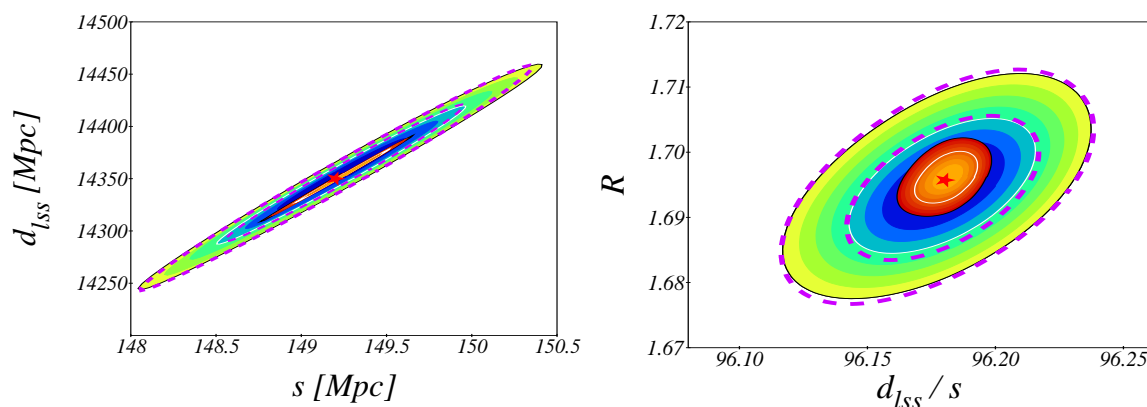


Figure 11. *Left panel:* CMB data determines the geometric quantities of the distance to last scattering d_{ls} and the sound horizon scale s precisely, and their ratio (the slope of the contours) – the acoustic peak angle – even more so. The contours give the 68.3% (white line) and 95.4% (black line) confidence levels for a cosmic variance limited experiment. Outer (dark blue to light green) contours use the temperature power spectrum, with dashed contours restricted to multipoles $\ell \geq 40$, while the inner (light gold to dark red) contours include the E -mode polarization and TE cross-spectrum. *Right panel:* Similar contours for the shift parameter $R = \sqrt{\Omega_m h^2} d_{\text{ls}}$ and acoustic peak scale.

The tightly constrained geometric information means that certain combinations of cosmological parameters are well determined, but this can actually be a pitfall if one is not careful in interpretation. Under certain circumstances, one such parameter is the value of the dark energy equation of state at a particular redshift, $w_\star = w(z \approx 0.4)$, related to a so-called pivot redshift. If CMB data is consistent with a cosmological constant universe, Λ CDM, then this forces $w_\star \approx -1$. However, this does not mean that dark energy is the cosmological constant – that is merely a mirage as a wide variety of dynamical models would be forced to give the same result. See §5.2 for further discussion.

3.4. Baryon acoustic oscillations

The sound horizon imprinted in the density oscillations of the photon-baryon fluid, showing up as acoustic peaks and valleys in the CMB temperature power spectrum, also appears in the large scale spatial distribution of baryons. Since galaxies, galaxy clusters, and other objects containing baryons can be observed at various redshifts, measurements of the angular scale defined by the standard ruler of the sound horizon provide a distance-redshift probe. Table 1 compares the acoustic oscillations in baryons and photons.

Table 1. Comparison of signals from perturbations in the prerecombination coupled baryon-photon fluid.

	Photons	Baryons
Effect	CMB acoustic peaks	Baryon acoustic oscillations
Scale	1°	$100 h^{-1}$ Mpc comoving
Base amplitude	5×10^{-5}	10^{-1}
Oscillation amplitude	$\mathcal{O}(1)$	5%
Detection	10^{15} /hand/sec	indirect: light from $< 10^{10}$ galaxies

For spatial density patterns corresponding to baryon acoustic oscillations (BAO) transverse to the line of sight, this is an angular distance relation while radially, along the line of sight, this is a proper distance interval, corresponding in the limit of small interval to the inverse Hubble parameter since $dr_{\text{prop}} = dz/[(1+z)H]$. It is important to remember that the quantities measured are actually distance ratios, i.e. $\tilde{d} = d_a/s$ and $\tilde{H} = sH$. These give different dependencies on the cosmological parameters than SN distances, as rather than being ratios relative to low redshift distances they are ratios relative to the high redshift universe (see §3.1 and Figures 7-8).

The BAO scale was first measured with moderate statistical significance in 2005 with Sloan Digital Sky Survey data [48, 49, 50] and 2dF survey data [51]. Current precision is 3.6% on the angular distance measurement at $z = 0.35$ and 6.5% at $z = 0.5$. Comparing the $z = 0.35$ SDSS result with the 2dF result at $z = 0.2$ reveals some tension [52], likely between the data sets [53] rather than from major deviation from the Λ CDM model. Note that the quantities quoted to date are not individual reduced distances but rather a roughly spherically averaged quantity convolving angular distance and proper distance interval.

To obtain the proper distance interval, and hence nearly the reduced Hubble parameter, requires accurate spectroscopic information to avoid projection of modes along the line of sight. Photometric redshifts allow estimation of the reduced angular distance but even that is at reduced precision until the redshift resolution approaches spectroscopic quality [54]. Since the sound horizon scale is about 1/30 of the Hubble radius today, assembling sufficient statistics to measure accurately the subtle signal

requires huge numbers of baryon markers over great volumes (10^6 - 10^9 over 1-100 Gpc³). For early papers on the cosmological use of BAO and issues regarding the interpretation of data, see [55, 56, 57, 58, 59, 60, 61, 62, 63, 64, 65].

3.5. Other methods

Many other probes of the expansion history and cosmic acceleration have been suggested, in the geometry, geometry+mass, or geometry+mass+gas categories. However many of them either lack a robust physical foundation or have yet to achieve practical demonstration of cosmological constraints. We therefore merely list some of the geometric methods with a few brief comments.

General tests of the expansion – These are in a certain sense the most fundamental and interesting. One well known test is that the CMB temperature should evolve with redshift as $T \sim 1 + z$. This depends on the phase space density of the radiation being conserved, following Liouville’s Theorem, e.g. photons do not convert into axions or appreciably interact with other components not in equilibrium with the radiation. It also requires the expansion to be adiabatic. Measurements to date, out to $z = 3$, show agreement with $T \sim 1 + z$ at modest precision, and further prospects include using the Sunyaev-Zel’dovich effect (Compton upscattering) in clusters to sample the radiation field seen by galaxy clusters at different redshifts [66].

Another test depending on Liouville conservation is the thermodynamic, or reciprocity, relation that can be phrased as a redshift scaling between angular distances and luminosity distances or “third party” angular distances between points not including the observer. Most commonly the relation is written as $d_l = (1 + z)^2 d_a$. This has a long history in cosmology, dating from the 1930s with Tolman [67], Ruse [68], and Etherington [69], through the 1970s with Weinberg [70], and a general proof in terms of the Raychaudhuri equation and the second law of thermodynamics by [71, 31]. The thermodynamic connection is basically that if two identical blackbodies sent photons to each other in a cyclic process over cosmic distances then work would be done unless the relation holds.

While the generality of these two probes as tests of the nature of the expansion itself is intriguing, if a violation were found one might be far more likely to blame uncertainties in the sources than a radical breakdown of the physics.

Epochs of the expansion – The expansion history can also be probed at certain special epochs. For example, light element abundances are sensitive to the expansion rate during primordial nucleosynthesis [72]. The CMB recombination epoch and sound horizon are influenced by deviations from matter and radiation dominated expansion [73, 74]. In the future, if we measure the abundance and mass of dark matter particles as thermal relics, we may be able to constrain the expansion rate at their freezeout epoch near perhaps 1 TeV ($z = 10^{16}$) [75]. Such early constraints are particularly interesting in multifield or multiepoch acceleration models [76].

Gamma ray bursts – As sources detectable to high redshift and insensitive to

dust extinction, some hope existed that gamma ray bursts could serve as standardized candles to high redshift (but see §3.6 and Figure 12 regarding the limited leverage of high redshift). However, while SN have an intrinsic flux dispersion of less than 50% that one calibrates down to 15% scatter, GRBs start with an isotropic-equivalent energy dispersion of a factor 1000, making any calibration much more challenging. Standardization relations were often ill defined and sensitive to environment [77] and with better data it is now realized that much of the correlation arose from experimental selection effects [78].

Gravitational wave sources – The intrinsic amplitude of clean systems like inspiraling black hole binaries can be predicted from observations of the gravitational waveform, giving a standard siren to compare to detected gravitational wave amplitude, thus providing a distance [79, 80]. No such observations have yet been achieved. Obtaining the redshift part of the distance-redshift relation depends on observing an electromagnetic counterpart.

Gravitational lensing cosmography – Deflection of light by massive objects depends on the mass distribution, the distances of source and lens from the observer, and the laws of gravity. However, cross-correlation techniques between sources at different redshifts have been proposed to reduce the need for knowing the mass distribution to extract distances [81, 82, 83]. Practical demonstration has not yet occurred.

Environment dependent methods – Techniques that intrinsically depend on not just a single source but its environment or group properties require greater understanding of many astrophysical factors. Such techniques often have not yet established a clear or robust physical motivation for the standardization essential to a distance probe. Approaches attempted include the galaxy age-redshift relation [84, 85, 86], active galactic nuclei radio jets [87], active galactic nuclei reverberation mapping [88, 89], and starburst galaxies [90].

3.6. Summary of mapping techniques

- To map the cosmological expansion accurately requires clear, robust, mature measurement techniques.
- Observations over a range of redshifts are required to break degeneracies, or equivalently rotate likelihood contours. Complementary probes do this as well.
- Systematics control can narrow contours and prevent biases in parameter estimation; see §5 for further analysis and discussion.

We have seen that much of the leverage for mapping the cosmic expansion is determined by the innate cosmology dependence on the parameters, and any survey design must work within this framework. One implication of this is that there is a survey depth of diminishing returns; beyond some redshift $z \approx 2$ little additional leverage accrues to measuring such high redshift distances relative to low redshift distances. That is, although the lever arm is longer, the lever is weaker. For high redshift

distances measured relative to the high redshift universe, the lever arm is shorter, so again improvement in constraints stalls at high redshift.

Figure 12 illustrates that once the expansion history is determined out to, say, $z \approx 1.5$ (or $2/3$ the age of the universe) that it is exceedingly difficult to measure geometrically more about dark energy with any significance. Even the simple question of whether the equation of state has *any* deviation from the cosmological constant requires percent level accuracy. Note that at high redshift the range $w \in [-\infty, 0]$ is comprehensive in that $w = -\infty$ means the dark energy density contributes not at all, and $w > 0$ would mean it upsets matter domination at high redshift (limits on this are discussed further in §4.1). Thus distance probes of the expansion history are driven organically by cosmology to cover the range from $z = 0$ to 1.5 – 2 .

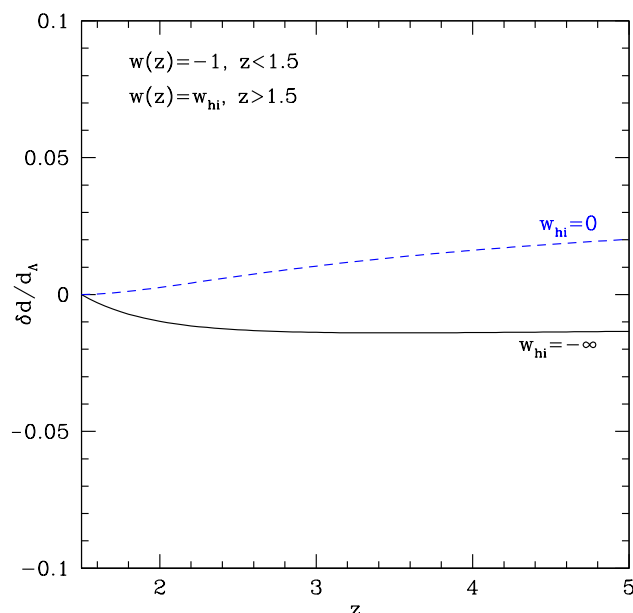


Figure 12. Once the most recent two-thirds of the cosmological expansion is determined, deeper measurements of distances tied to low redshift have little further leverage. Over the physically viable range for the high redshift dark energy equation of state $w \in [-\infty, 0]$, distances do not vary between models by more than 1-2%, exceedingly difficult to measure accurately at high redshift. Cosmological considerations alone indicate that covering the range out to $z = 1.5$ – 2 is the optimal strategy.

4. Growth and expansion

Within the theory of general relativity, the cosmic expansion history completely determines the growth of matter density perturbations on large scales. On smaller scales the state of the matter, e.g. the Jeans length defined by pressure effects, enters as well and when density fluctuations go nonlinear then radiative and gas heating and

cooling, star formation, feedback etc. affect the formation and evolution of structure. Here we consider only the large scale, linear regime and the role that growth observations can play in mapping the cosmological expansion.

4.1. Growth of density perturbations

For a matter density perturbation $\delta\rho$, its evolution is reduced from the Newtonian exponential growth on the gravitational dynamical timescale $t_{\text{dyn}} = 1/\sqrt{G\rho}$ to power law growth on a Hubble timescale by the drag induced from the cosmological expansion. Generally,

$$g'' + \left[4 + \frac{1}{2}(\ln H^2)'\right] g' + \left[3 + \frac{1}{2}(\ln H^2)' - \frac{3}{2}\Omega_m(a)\right] g = 0, \quad (9)$$

where $g = (\delta\rho/\rho)/a$ is the normalized growth, a prime denotes differentiation with respect to $\ln a$, and the dimensionless matter density $\Omega_m(a) = \Omega_m a^{-3}/[H/H_0]^2$. Thus the growth indeed depends only on the expansion history H (the matter density is implicit within the high redshift, matter dominated expansion behavior).

In a matter dominated epoch, the solution is $\delta\rho/\rho \sim a$, so we defined g such that it would be constant (which we can arrange to be unity) in such a case. In an epoch dominated by an unclustered component with equation of state w , matter density perturbations do not grow. Note that this is due to the small source term, not the Hubble drag – indeed the Hubble drag term is proportional to $5 - 3w$ and is less strong in a radiation dominated universe than a matter dominated universe, yet matter density perturbations still do not grow in the radiation epoch. If one somehow fixed $\Omega_m(a)$ as one changed w , then increasing w indeed aids growth. For domination by a component with $w < 0$ (not acceleration per se) there is the double whammy of reduced source term and increased friction.

As the universe makes the transition from being dominated by a $w > 0$ component to matter domination, the solution is

$$\delta\rho/\rho \sim 1 + \frac{\Omega_m}{\Omega_w} \frac{1}{w(1+3w)} a^{3w}. \quad (10)$$

One can see the transition from no growth $\delta \sim \text{constant}$ to growth (with $\delta \sim a$ for a radiation-matter transition). For a transition from matter domination to being dominated by a $w < 0$ component, to first order

$$\delta\rho/\rho \sim a \left[1 - \frac{1-w}{-w(5-6w)} \frac{\Omega_w}{\Omega_m} a^{-3w}\right]. \quad (11)$$

Finally, for a $w = 0$ component that does not behave in the standard fashion, e.g. a constant fraction F of the matter density does not clump, then

$$\delta\rho/\rho \sim a^{(\sqrt{25-24F}-1)/4}. \quad (12)$$

For example, a small fraction Ω_e of early dark energy with $w = 0$ leads to $\delta\rho/\rho \sim a^{1-(3/5)\Omega_e}$ at early times. See [91, 92, 9] for early discussion of these growth behaviors in multicomponent universes.

Since the origin of the density perturbation source term is the Poisson equation, basically contributing $4\pi G_N \delta\rho$, any modification to this equation gives an effective $F(k, a) \equiv [G\Omega_m(k, a)]/[G_N\Omega_m(a)]_{\text{std}}$ that produces modified growth, where the wavenumber k allows for spatially dependent modifications. If F is nearly constant in time, then the growth is determined by Eq. (12). However, if the physical origin of the modification also affects the expansion, as from a time dependent gravitational coupling G_N , then one must alter the other growth equation terms as well to obtain the solution.

Growth measurements, being integrals from high redshift, can probe the high redshift universe. For example, a measurement of the growth factor at, say, $z = 2$ that agrees with a Λ CDM model mapped out at lower redshift ensures that the high redshift epoch of matter domination occurred substantially as expected. Specifically, if the linear growth factor at $z = 2$ deviates by less than 5%, then for a monotonically varying dark energy model described by $w(a) = w_0 + w_a(1 - a)$, we can limit $w_a < 0.6$ or $w(z = 2) < -0.6$. We can also constrain an intermediate, transient epoch of acceleration in the cosmic expansion. Growth measurements can place tight constraints on this mechanism for easing the coincidence problem [93], as shown in Figure 13. To prevent strong deviations in growth that would be evident in measurements, the period of such acceleration must be much shorter than the characteristic Hubble timescale (and hence apparently “unnatural”).

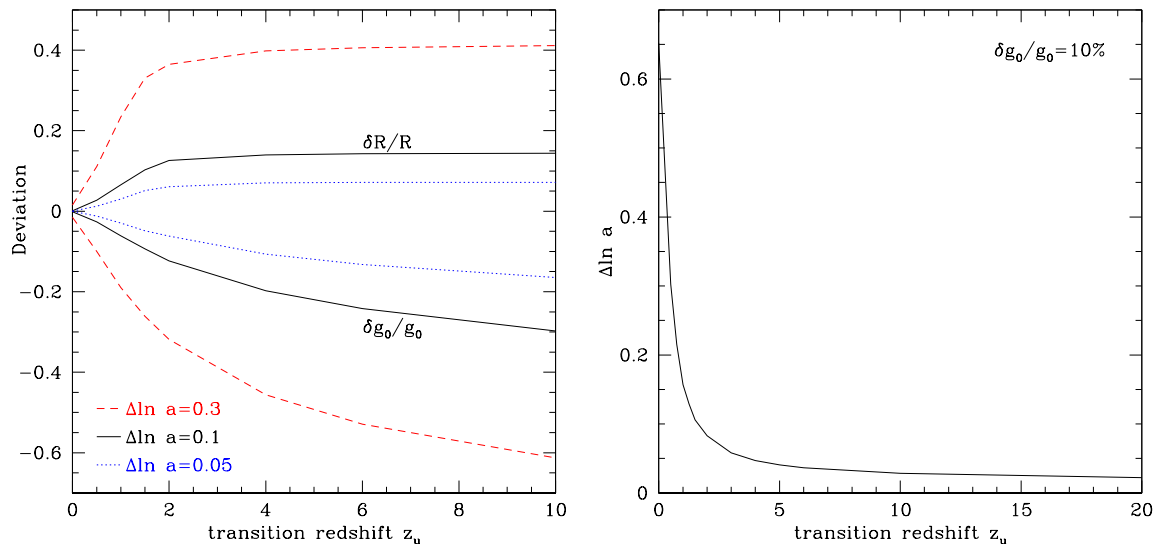


Figure 13. Growth measurements can strongly constrain events in the cosmological expansion such as an intermediate epoch of acceleration. The left panel show the deviations from the Λ CDM growth, in the present total growth g_0 and growth ratio $R = g(a = 0.35)/g_0$, for a transition to total equation of state -1 lasting a period $\Delta \ln a$, ending at redshift z_u . The right panel shows the limit on the length of the acceleration allowed as a function of transition redshift, in order for deviations to the total growth to be less than 10%.

Overall, the growth history has the potential to constrain the expansion history. However, there are some obstacles. The growth also depends on the initial conditions, couplings to other components, and deviations of gravity from general relativity. For example, in a radiation dominated universe growth should not occur, but if the perturbation evolution has some “velocity” from a previous matter dominated epoch it can proceed with a slow, $\ln a$ growth. (Similarly, growth persists into an accelerating epoch.) Another example is that in the prerecombination universe baryons were tightly coupled to photons, preventing growth [94]. Finally, it is quite difficult to detect the matter perturbations per se, instead we observe light from galaxies – a biased tracer of the density field. Separating the absolute growth factor from the bias, or the relative growth from an evolution in bias, is nontrivial [95].

Measurements of growth are therefore presently not clean probes of the expansion history, especially since, as Eq. (9) indicates, precision knowledge of Ω_m is required to truly use this approach to map $H(z)$. Redshift distortion measurements of the growth of the matter velocity field (rather than density), employing $d \ln g / d \ln a$, have similar issues. See [96, 97] for good overviews of the current status of growth measurements.

4.2. Abundance tests

Under gravitational instability, mass aggregates and galaxies and clusters of galaxies form, evolving in number and mass. The abundance as a function of redshift of particular classes of objects will involve (among other variables) the initial power spectrum, astrophysical processes such as dissipation and feedback, and the expansion rate of the universe, as well as a robust observational proxy for mass. Two famous examples of using galaxy abundances as cosmological probes are in a 1975 paper “An Accelerating Universe” [98] and in 1986 “Measurement of the Mass Density of the Universe” [99]. As the titles suggest, the data led to opposite conclusions and each was quickly recognized to be showing more about astrophysical evolution of the objects than the cosmological expansion history.

New generations of experiments are underway to count sources as a function of redshift and mass, selecting samples through their detection in the Sunyaev-Zel’dovich effects, X-ray flux, optical flux, or weak gravitational lensing shear. Currently, data is insufficient to give robust cosmological constraints on the expansion history. Note that observations do not actually measure an abundance per comoving volume, $dN(m)/dV$, which would show how structures grow in mass while their (nonevolving) numbers should stay constant. Rather they see dN/dz which involves distances through an extra factor of dV/dz . Thus observed abundances do not give a pure growth probe but mix geometry and growth – both an advantage and disadvantage.

4.3. Gravitational lensing

The gravitational potentials of massive structures deflect, focus, and shear bundles of light rays from more distant sources. The particular shear pattern combines

information from both the lensing mass and the “focal length” defined by the source and lens distances from the observer. To date, most such data provides leverage on a combination of the matter density Ω_m and the rms amplitude of mass fluctuations σ_8 . A few surveys so far quote further cosmological constraints – on the dark energy parameters in combination with other data sets [100], or on the presence of growth [101, 102, 103, 104, 105].

A number of interesting concepts for using gravitational lensing to map the cosmological expansion exist, though practicality has yet to be demonstrated. Both the magnification or convergence fields and the shear field carry cosmological information. For use as a geometric probe, one must separate astrophysical or instrumental effects, deconvolve the lens gravitational potential model, and measure the redshifts or redshift distribution of the lenses and sources accurately. See [81, 82, 83] for discussion of weak lensing as a geometric probe. Lensing of the CMB, where the source redshift is known, is another interesting application [106]. In theory, if one could separate out the distances and other factors, one could also probe the growth history.

4.4. Testing gravity

4.4.1. First steps Although the focus of this article is on mapping the cosmological expansion, since the growth history depends on both the expansion and the laws of gravity one could consider using expansion plus growth measurements to test the gravitational framework. This is an exciting possibility that has recently received considerable attention in the literature (see, e.g., [107, 37, 108, 109] for early work), although current data cannot provide significant constraints.

In addition to comparing predictions of specific theories of gravity to data, one basic approach is parametrization of gravitational cosmological effects. While one could define cosmological parameters $\Omega_m^{\text{gr}}, w_0^{\text{gr}}, w_a^{\text{gr}}$, say, derived from fitting the growth history and contrast these with those derived from pure expansion measurements, one could also keep the physics of cosmic expansion expressed through the well-defined (effective) parameters Ω_m, w_0, w_a and look for physical effects from gravity beyond Einstein relativity in separate, clearly interpretable gravitational parameters.

The gravitational growth index γ was designed specifically to preserve this distinction of physical phenomena [110]. Here the matter density linear growth factor $g = (\delta\rho/\rho)/a$ is written

$$g(a) = e^{\int_0^a (da'/a') [\Omega_m(a')^\gamma - 1]}. \quad (13)$$

See [110, 111, 112] for discussion of the accuracy, robustness, and basis of this form. However, gravity does more than affect the growth: it affects the light deflection law in lensing and the relation between the matter density and velocity fields. Since two potentials enter generically, in the time-time and space-space terms of the metric, [113, 114, 115, 116, 117, 118] and others have proposed two or more parameters for testing extensions to general relativity (GR). These may involve the ratio of metric

potentials (unity for GR), as a cosmological generalization of the parametrized post-Newtonian quantity, and their difference (zero for GR), related to the anisotropic stress.

4.4.2. Problems parametrizing beyond-Einstein gravity The two gravitational parameter approach is an exciting idea that deserves active exploration. Here, however, to balance the literature we undertake a more critical overview of this program. Difficulties to overcome include:

- (i) Reduction of two functions to two (or a small number) of parameters;
- (ii) Spatial dependence, e.g. strong coupling or Vainshtein scales, or quantities living in real space vs. Fourier space;
- (iii) Covariance among deviations in gravitational coupling, metric potentials, and fluid anisotropic stress.

We give very brief assessments of each item. For the first point, a successful proof of concept is the gravitational growth index, which for a wide class of theories adds a single (constant) parameter to describing linear growth. [112] explains why this works under certain conditions, basically requiring small deviations from standard cosmological expansion and gravity. Many theories indeed have small deviations, but these are often so small they become problematic to detect; other theories with larger deviations are either ruled out by, e.g., solar system tests or have scale dependence requiring multiple parameters.

Regarding the second point, in the parametrized post-Newtonian (PPN) formalism the ratio of metric potentials is defined in real space, e.g. $\Phi(r)/\Psi(r)$. This is not equivalent to defining a parameter $\eta = \Phi_k/\Psi_k$ in Fourier space. Given some function $f(r) = \Phi(r) + \Psi(r)$, it is not generically true that a nonlinear function $F(f(r))$ depends in the same manner on Φ and Ψ . Thus many power spectra, e.g. involving $\langle(\Phi + \Psi)^2\rangle$ for the integrated Sachs-Wolfe effect, will not follow the simple formalism.

Spatial variation also does not preserve the functional dependence; for example, while the light deflection angle depends on the specific combination $\Phi(r) + \Psi(r)$, the actual deflection at impact parameter b is not a function only of $\Phi(b) + \Psi(b)$. Consider lensing in DGP [119] gravity, where

$$\Phi(r) = \frac{m}{r} + \frac{n_\phi}{r^3} \tag{14}$$

$$\Psi(r) = \frac{m}{r} + \frac{n_\psi}{r^3} \tag{15}$$

where the n 's are related to extradimensional quantities. (Many IR modifications of gravity have this form, but note it is very different from the Yukawa form so general parametrization of spatial dependence may be difficult). Thus $f(r)$ takes the form $2m/r + n/r^3$ and some function, say,

$$F(f(r_0)) = \int_{r_0}^{\infty} \frac{dr}{r} f(r) = \frac{2m}{r_0} + \frac{n}{3r_0^3} \neq C [\Phi(r_0) + \Psi(r_0)], \tag{16}$$

for any constant C . More concretely, for deflection of light at impact parameter b from a point mass (extending [120]), we find the deflection angle

$$\alpha_b = 2 [\Phi + \Psi]_b - 6 [\Psi - \Phi]_b, \quad (17)$$

breaking the functional form $\Phi + \Psi$ with an extra term looking like a spurious anisotropic stress. Thus observations of lensing deflection do not tell us about a simple parameter η in the form $\Phi (1 + \eta)$, as we might hope.

Another issue concerns interdependence among different aspects of gravitational modifications. Variation in gravitational coupling may well occur alongside anisotropic stress, as in scalar-tensor theories. In Poisson’s equation, therefore, one cannot define a Fourier space mass power spectrum $\langle \delta_k^2 \rangle$ because the physical source involves $\langle (G_{\text{eff}} \delta_k)^2 \rangle$ and it may not be clear how the interaction of these two quantities affects the result. This is reminiscent of varying constant theories where one can calculate the effects of a varying fine structure constant, say, but does not have a unified framework for understanding how the electron-proton mass ratio, say, varies simultaneously, and hence affects observations as well [121]. Confusion also arises between gravitational modifications and fluid microphysics, e.g. anisotropic stress of a component, coupling between components, or finite sound speed (see, e.g., [122]).

4.4.3. Levels of discovery In summary, there is a rich array of challenges for a program seeking to parameterize beyond Einstein gravity. One ray of hope is that different observations depend differently on the quantities, some of which are outlined in Table 2 (also see [118]). And of course SN are possibly unique in being pure geometric probes of the cosmological expansion, immune to the uncertainties imposed by these additional parameters (even $G(t)$, see e.g. [127]), providing the clearest, most unambiguous understanding. We emphasize this point: all other methods in use rely on understanding the rest of the dark sector – dark matter and gravity – as they seek to explore dark energy. As well though, we should keep in mind the insight by Richard Feynman:

“Yesterday’s sensation is today’s calibration, and tomorrow’s background.”

Mapping the cosmological expansion with a simple, robust, and geometric method like supernovae provides a firm foundation from which to probe deeper, with techniques that have more complex – richer – dependence on further variables revealing the microphysics and testing gravity.

5. Systematics in data and theory

Accurate mapping of the cosmological expansion requires challenging observations over a broad redshift range with precision measurements. Technological developments such as large format CCDs, large telescopes, and new wavelength windows make such surveys possible. In addition to obtaining large data sets of measurements, we must also address

Table 2. Theory systematics occur even for some geometric probes, the cleanest astrophysically. For example, light deflection depends on the metric potentials as $\Phi + \Psi$, plus separating out the mass model, and baryon acoustic oscillations are sensitive to the validity of the usual CDM growth, hence affected by Φ and Ψ (see, for example, [123] for difficulties in the braneworld case), new density perturbations due to the sound speed c_s (see, e.g., [124]) and anisotropic stress π_s , variation of the gravitational coupling G with scale and time, and altered fluctuations due to matter coupling Γ (see, e.g., [125, 126]).

Probe	Theory Systematic (dominant)	Theory Systematic (potential)
SN Ia	—	—
WL	$\Phi + \Psi$	$c_s, \pi_s, G(k, t)$
BAO	Φ, Ψ, c_s, Γ	$\pi_s, G(k, t)$

systematic uncertainties in measurements and astrophysical source properties. Beyond that, for accurate mapping we must consider systematics in the theoretical interpretation and the data analysis. Here we present some brief illustrations of the impact of such systematics on mapping the expansion.

5.1. Parameterizing dark energy

In extracting cosmological parameters from the data, one wants parameters that are physically revealing, that can be fit precisely, and that accurately portray the key physical properties. For exploration of many different parametrizations and approaches see [18] and references therein. Any functional form for the expansion, e.g. the dark energy equation of state $w(z)$, runs the risk of limiting or biasing the physical interpretation, so one can also consider approaches such as binned equations of state, defined as tophats in redshift, say, or decomposition into orthogonal basis functions or principal component analysis (see, e.g., [128]). However, for a finite number of components or modes this does not solve all the problems, and introduces some new ones such as model dependence and uncertain signal-to-noise criteria (see [129] for detailed discussion of these methods).

Indeed, even next generation data restricts the number of well-fit parameters for the dark energy equation of state to two [130], greatly reducing the flexibility of basis function expansion or bins. Here, we concentrate on a few comments regarding two parameter functions and how to extract clear, robust physics from them.

For understanding physics, two key properties related to the expansion history and the nature of acceleration are the value of the dark energy equation of state and its time variation $w' = dw/d\ln a$. These can be viewed as analogous to the power spectral tilt and running of inflation. The two parameter form

$$w(a) = w_0 + w_a(1 - a), \quad (18)$$

based on a physical foundation by [40], has been shown to be robust, precise, bounded, and widely applicable, able to match accurately a great variety of dark energy physics.

See [131] for tests of its limits of physical validity.

One of the main virtues of this form is its model independence, serving as a global form able to cover reasonably large areas of dark energy phase space, in particular both classes of physics discussed in §2.3 – thawing and freezing behavior. We can imagine, however, that future data will allow us to zero in on a particular region of phase space, i.e. area of the w - w' plane, as reflecting the physical origin of acceleration. In this case, we would examine more restricted, local parametrizations in an effort to distinguish more finely between physics models.

First consider thawing models. One well-motivated example is a pseudoscalar field [132], a pseudo-Nambu Goldstone boson (PNGB), which can be well approximated by

$$w' = F(1 + w) \quad (19)$$

$$w(a) = -1 + (1 + w_0) a^F, \quad (20)$$

where F is inversely proportional to the PNGB symmetry breaking energy scale f . Scalar fields, however, thawing in a matter dominated universe, must at early times evolve along the phase space track $w' = 3(1 + w)$ [17], where w departs from -1 by a term proportional to a^3 . One model tying this early required behavior to late times and building on the field space parametrization of [133] is the algebraic model of [18],

$$1 + w = (1 + w_0) a^p \left(\frac{1 + b}{1 + ba^{-3}} \right)^{1-p/3}, \quad (21)$$

with parameters w_0, p ($b = 0.3$ is fixed). Figure 14 illustrates these different behaviors and shows matching by the global (w_0, w_a) model, an excellent approximation to $w(z)$ out to $z \gtrsim 1$. More importantly, it reproduces distances to all redshifts to better than 0.05%. The key point, demonstrated in [18], is that use of any particular one of these parametrizations does not bias the main physics conclusions when testing consistency with the cosmological constant or the presence of dynamics. Thus one can avoid a parametrization-induced systematic.

For freezing models, we can consider the extreme of the early dark energy model of [134], with 3% contribution to the energy density at recombination, near the upper limit allowed by current data [135]. This model is specifically designed to represent dark energy that scales as matter at early times, transitioning to a strongly negative equation of state at later times. If future data localizes the dark energy properties to the freezing region of phase space, one could compare physical origins from this model (due to dilaton fields) with, say, the H^α phenomenological model of [136] inspired by extra dimensions. Again a key point is that the global (w_0, w_a) parametrization does not bias the physical conclusions, matching even the specialized, extreme early dark energy model to better than 0.02% in distance out to $z \approx 2$.

Parametrizations to be cautious about are those that arbitrarily assume a fixed high redshift behavior, often setting $w = -1$ above some redshift. These can strongly bias the physics [129, 131]. As discussed in §2, interesting and important physics clues may reside in the early expansion behavior.

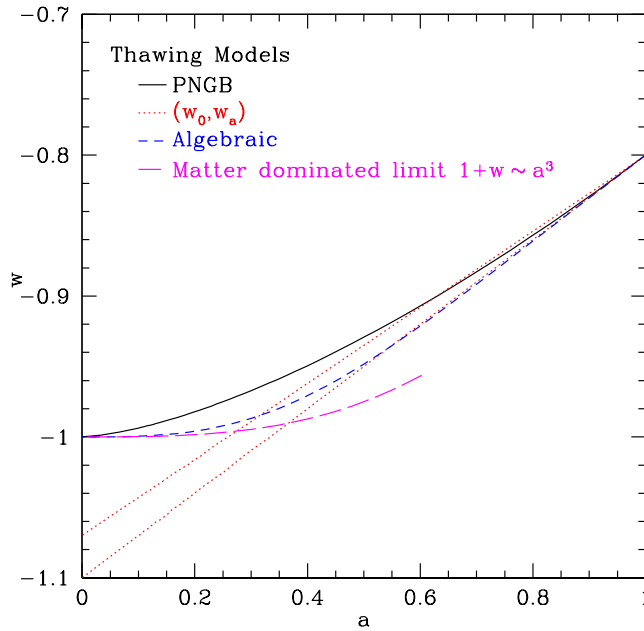


Figure 14. Within the thawing class of physics models one can hope to distinguish specific physics origins. A canonical scalar field evolves along the early matter dominated universe behavior shown by the “matter limit” curve, then deviates as dark energy begins to dominate. Such thawing behavior is well fit by the algebraic model. A pseudoscalar field (PNGB) evolves differently. Either can be moderately well fit by the phenomenological (w_0, w_a) parametrization for the recent universe.

Bias can also ensue by assuming a particular functional form for the distance or Hubble parameter [137]. Even when a form is not assumed a priori, differentiating imperfect data (e.g. to derive the equation of state) leads to instabilities in the reconstruction [138, 139]. To get around this, one can attempt to smooth the data, but this returns to the problems of assuming a particular form and in fact can remove crucial physical information. While the expansion history is innately smooth (also see §6.2), extraction of cosmological parameters involves differences between histories, which can have sharper features.

5.2. Mirage of Lambda

As mentioned in §3.3, interpreting the data without fully accounting for the possibility of dynamics can bias the theoretical interpretation. We highlight here the phenomenon of the “mirage of Λ ”, where data incapable of precisely measuring the time variation of the equation of state, i.e. with the quality expected in the next five years, can nevertheless apparently indicate with high precision that $w = -1$.

Suppose the distance to CMB last scattering – an integral measure of the equation of state – matches that of a Λ CDM model. Then under a range of circumstances, low redshift ($z \lesssim 1$) measurements of distances can appear to show that the equation of state

is within 5% of the cosmological constant value, even in the presence of time variation. Figure 15 illustrates the sequence of physical relations leading to this mirage.

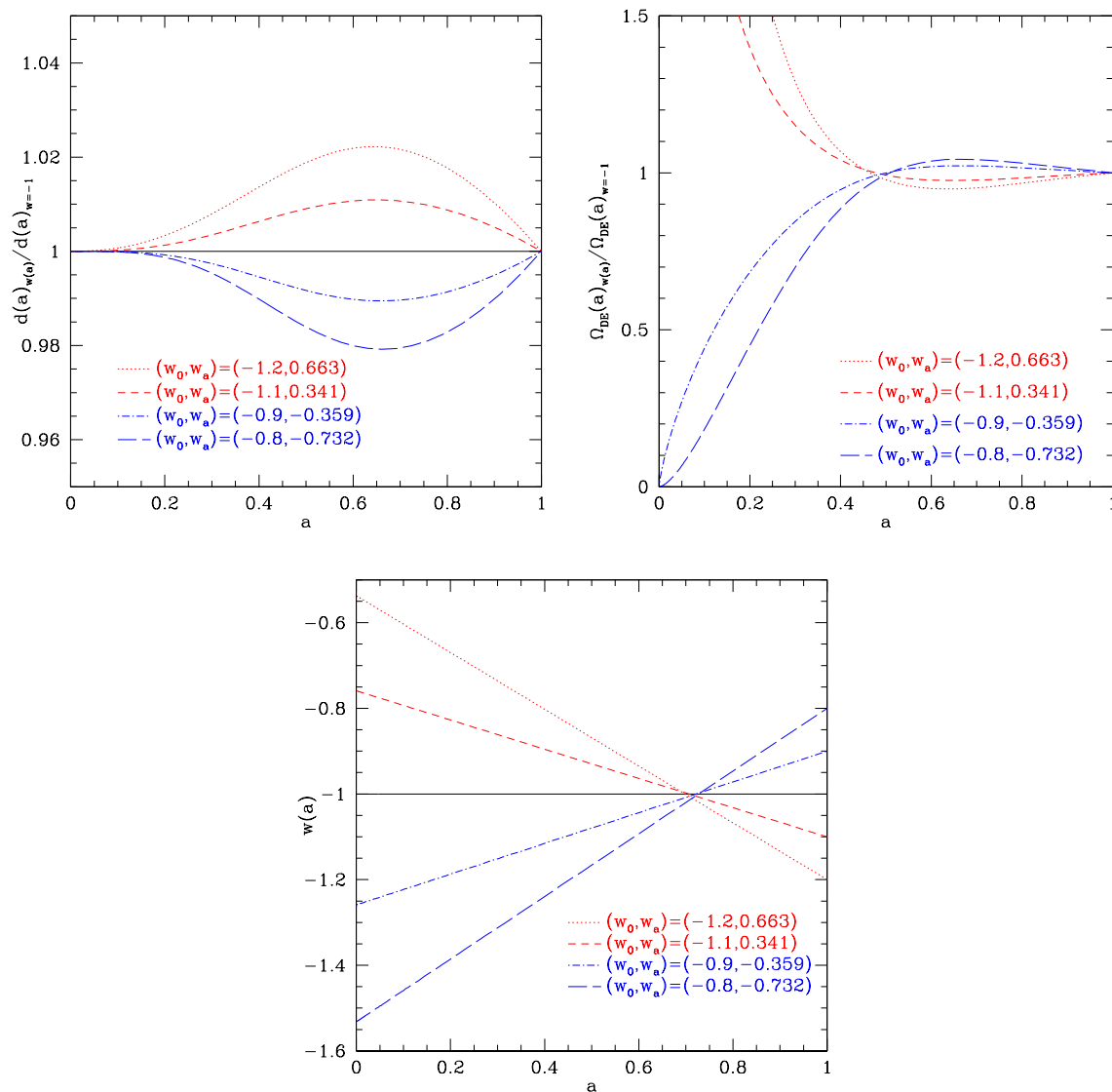


Figure 15. Matching the distance to CMB last scattering between dark energy models leads to convergence and crossover behaviors in other cosmological quantities. The top left panel illustrates the convergence in the distance-redshift relation, relative to the Λ CDM case, for models with w_0 ranging from -0.8 to -1.2 and corresponding time variation w_a . The top right panel illustrates the related convergence and crossover in the dark energy density $\Omega_{DE}(a)$, and the bottom panel shows how the CMB matching necessarily leads to a crossover with $w = -1$ at the key redshift for sensitivity of low redshift experiments. This crossover in $w(z)$ leads to the mirage of Λ , and is impelled by the physics not the functional form.

Matching the distance to last scattering imposes a relation between the cosmological parameters, here shown as a family of (w_0, w_a) models holding other parameters fixed.

The convergence in their distances beginning at $a \approx 0.65$ is associated with a similar convergence in the fractional dark energy density, and a matching in $w(z)$ at $a \approx 0.7$. Note that even models with substantial time variation, $w_a \approx 1$, are forced to have $w(z \approx 0.4) = -1$, i.e. look like the cosmological constant. This is dictated by the innate cosmological dependences of distance and is robust to different parameter choices; see [131] for more details. (Note the matching in $\Omega_{\text{DE}}(a)$ forced at $a \approx 0.5$ has implications for the linear growth factor and nonlinear power spectrum, as explored in [140].)

To see beyond the mirage of Λ , or test its reality, requires measurements capable of directly probing the time variation with significant sensitivity (hence extending out to $z \approx 1.7$ as shown in §3.1). Current and near term experiments that may show $w \approx -1$ to a few percent can induce a false sense of security in Λ . In particular, the situation is exacerbated by the pivot or decorrelation redshift (where the equation of state is measured most precisely) of such experiments probing to $z \approx 1$ being close to the matching redshift imposed on $w(z)$; so, given CMB data consistent with Λ , such experiments will measure $w = -1$ with great precision, but possibly quite inaccurately. See Figure 16 for a simulation of the possible data interpretation in terms of the mirage of Λ from an experiment capable of achieving 1% minimum uncertainty on w (i.e. $w(z_{\text{pivot}})$). Clearly, the time variation w_a is the important physical quantity allowing us to see through the mirage, and the key science requirement for next generation experiments.

5.3. Inhomogeneous data sets

Turning from theory to data analysis, another source of systematics that can lead to improper cosmological conclusions are heterogeneous data sets. This even holds with data all for a single cosmological probe, e.g. distances. Piecing together distances measured with different instruments under different conditions or from different source samples opens the possibilities of miscalibrations, or offsets, between the data.

While certainly an issue when combining, say, supernova distances with baryon acoustic oscillation distances, or gravitational wave siren distances, we illustrate the implications even for heterogeneous supernova samples. An offset between the magnitude calibrations can have drastic effects on cosmological estimation (see, e.g., [141]). For example, very low redshift ($z < 0.1$) supernovae are generally observed with very different telescopes and surveys than higher redshift ($z > 0.1$) ones. Since the distances in the necessary high redshift ($z \approx 1 - 1.7$) sample require near infrared observations from space then the crosscalibration with the local sample (which requires very wide fields and more rapid exposures) requires care. The situation is exacerbated if the space sample does not extend down to near $z \approx 0.1 - 0.3$ and a third data set intervenes. This gives a second crosscalibration needed to high accuracy.

Figure 17 demonstrates the impact on cosmology, with the magnitude offset leading to bias in parameter estimation. If there is only a local distance set and a homogeneous space set extending from low to high redshift, with crosscalibration at the 0.01 mag

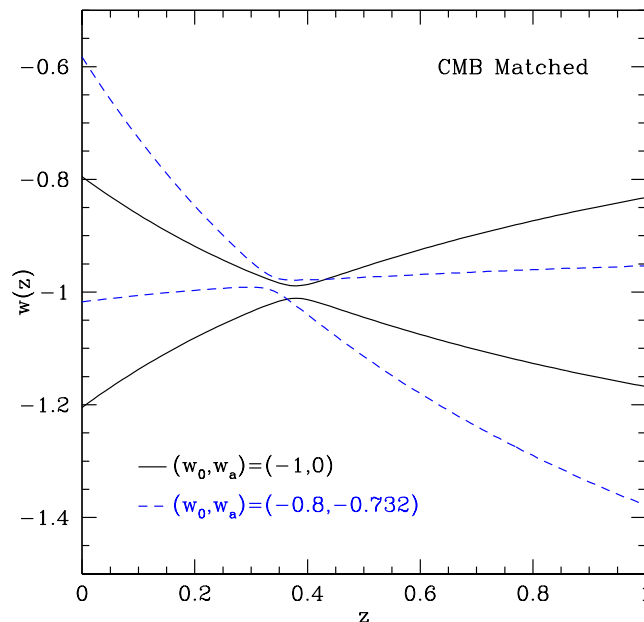


Figure 16. If CMB data are consistent with Λ CDM, this can create a mirage of Λ for lower redshift distance data even if the dark energy has substantial time variation. The curves show simulated 68% confidence regions for $w(z)$ for two different CMB-matched models. The value of the equation of state $w(z) = -1$ necessarily, for each one at a redshift close to the “sweet spot” or pivot redshift. Experiments insufficiently precise to see time variation will think $w = -1$ to high precision (the width of the narrow waist at $z \approx 0.38$, here 1%) even if the true behavior is drastically different.

level, then the biases take on the values at the left axis of the plot: a small fraction of the statistical dispersion. However, with an intermediate data set, the additional heterogeneity from matching at some further redshift z_{match} (with the systematic taken to be at the 0.02 mag level to match a ground based, non-spectroscopic experiment to a space based spectroscopic experiment) runs the risk of bias in at least one parameter by of order 1σ . Thus cosmological accuracy advocates as homogeneous a data set as possible, ideally from a single survey.

Similar heterogeneity and bias can occur in baryon acoustic oscillation surveys mapping the expansion when the selection function of galaxies varies with redshift. If the power spectrum shifts between samples, due for example to different galaxy-matter bias factors between types of galaxies or over redshift, then calibration offsets in the acoustic scale lead to biases in the cosmological parameters. Again, innate cosmology informs survey design, quantitatively determining that a homogeneous data set over the redshift range is advantageous.

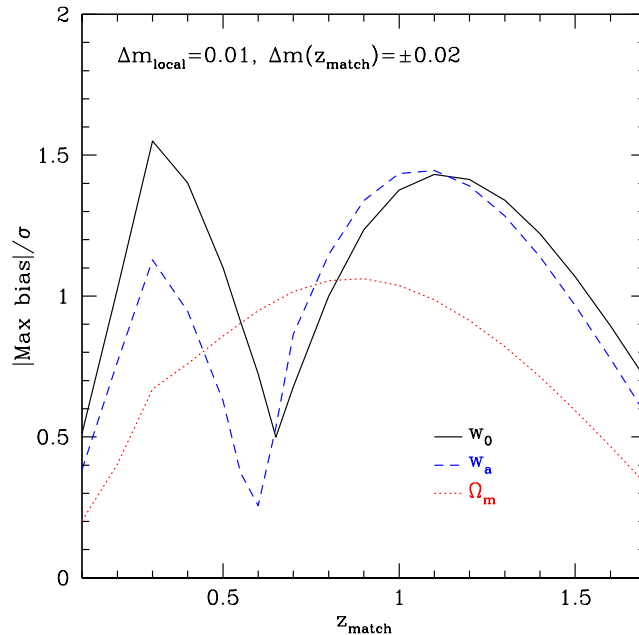


Figure 17. Heterogeneous datasets open issues of imperfect crosscalibration, modeled here as magnitude offsets Δm . One scenario involves calibration between a local ($z < 0.1$) spectroscopic set and a uniform survey extending from $z \approx 0.1 - 1.7$. This imposes cosmological parameter biases given by the intersection of the curves with the left axis. Another scenario takes the high redshift data to consist of two, heterogeneous sets with an additional offset Δm at some intermediate matching redshift z_{match} . (When $z_{\text{match}} = 0.1$ this corresponds to the first scenario with no extra offset.)

5.4. Miscalibrated standard

Miscalibration involving the basic standard, i.e. candle luminosity or ruler scale, has a pernicious effect biasing the expansion history mapping. This time we illustrate the point with baryon acoustic oscillations. If the sound horizon s is improperly calibrated, with an offset δs (for example through early dark energy effects in the prerecombination epoch [142, 143]), then every baryon acoustic oscillation scale measurement $\tilde{d}(z) = d(z)/s$ and $\tilde{H}(z) = sH(z)$ will be miscalibrated. Due to the redshift dependence of the untilded quantities, the offset will vary with redshift, looking like an evolution that can be confused with a cosmological model biased from the reality.

To avoid this pitfall, analysis must include a calibration parameter for the sound horizon (since CMB data does *not* uniquely determine it [144, 143]), in exact analogy to the absolute luminosity calibration parameter \mathcal{M} required for supernovae. That is, the standard ruler must be standardized; *assuming* standard CDM prerecombination for the early expansion history blinds the analysis to the risk of biased cosmology results.

The necessary presence of a standard ruler calibration parameter, call it \mathcal{S} , leads to an increase in the w_0 - w_a contour area, and equivalent decrease in the “figure of merit”, by a factor 2.3. Since we do not know a priori whether the high redshift universe is

conventional CDM (e.g. negligible early dark energy or coupling), neglecting \mathcal{S} for BAO is as improper as neglecting \mathcal{M} for supernova standard candle calibration. (Without the need to fit for the low redshift calibration \mathcal{M} , SN would enjoy an improvement in “figure of merit” by a factor 1.9, similar to the 2.3 that BAO is given when neglecting the high redshift calibration \mathcal{S} .)

For supernovae, in addition to the fundamental calibration of the absolute luminosity, experiments must tightly constrain any evolution in the luminosity [145]. This requires broadband flux data from soon after explosion to well into the decline phase, and spectral data over a wide frequency range. Variations in supernova properties that do not affect the corrected peak magnitude do not affect the cosmological determination.

5.5. Malmquist bias

Distance measurements from the cosmological inverse square law of flux must avoid threshold effects where only the brightest sources at a given distance can be detected, known as Malmquist bias. Suppose the most distant, and hence dimmest, sources were close to the detection threshold. We can treat this selection effect as a shift in the mean magnitude with a toy model,

$$\Delta m = -A \frac{z - z_\star}{0.95 - z_\star}, \quad z > z_\star. \quad (22)$$

This then propagates into a bias on the cosmological parameter fit to the data.

Consider a data set of some 1000 supernovae from $z = 0-1$, with the Malmquist bias setting in at $z_\star = 0.8$ (where ground based spectroscopy begins to get quite time intensive and many spectral features move into the near infrared). The bias in a cosmological parameter relative to its uncertainty is then

$$\frac{\delta p}{\sigma_p} = (1.5, 1.0, 1.2) \times \frac{A}{0.1 \text{ mag}} \quad (23)$$

for $p = (\Omega_m, w_0, w_a)$. Thus, the Malmquist bias must be limited to less than 0.05 mag at $z = 0.95$ to prevent significant bias in the derived cosmological model. In fact, this is not a problem for a well designed supernova survey since the requirement of mapping out the premaximum phase of the supernova ensures sensitivity to fluxes at least two magnitudes below detection threshold.

5.6. Other issues

In addition to the theory interpretation and data analysis systematics discussed in this section, recall the fundamental theory systematics of §4.4.3 and Table 2. We finish with a very brief mention of some other selected data and data analysis systematics issues of importance that are often underappreciated and that must be kept in mind for proper survey design and analysis.

- *Sample variance:* Along a given line of sight, the local distance measures anchoring the Hubble diagram can be influenced by coherent velocity flows, throwing off the derived cosmology [146, 147, 148]. The local distances should therefore be well into the Hubble flow and the sources distributed widely on the sky. In addition, the mass distribution along the line of sight may not be representative of the homogeneous model and gravitational lensing can lead to coherent magnification effects (relevant for standardized candles) and alterations of the measured three dimensional clustering (important for baryon acoustic oscillations). See, e.g., [149, 150]. For these reasons and others, “pencil beam” surveys can be fraught with systematics and are poor survey design.
- *Analytic marginalization:* The calibration parameter, e.g. \mathcal{M} combining the absolute luminosity and Hubble constant in the case of supernovae, is often referred to as a nuisance parameter but its proper treatment is essential. Although in some χ^2 formulas for the distance-redshift relation it is not written explicitly, it is implicit and cannot be ignored. More subtle is the issue of analytic marginalization over it – this must be used with great care (or, better yet, not used) as the distribution of \mathcal{M} is actually non-Gaussian due to interaction with other supernovae peak magnitude fitting quantities (such as the lightcurve width and color terms) [43]. Further subtleties exist between marginalization and minimization in a multidimensional fit space [151, 148], and most analysis from raw data to quoted parameters actually employs minimization techniques.
- *Extinction priors:* Since the dimming and reddening due to dust effects on supernovae are one-sided (i.e. dust does not increase the flux), they are highly non-Gaussian and must be treated with care. Any deviation between an assumed prior for extinction and the truth, that is not constant in redshift, can bias the cosmology results. See Figure 18 and the handy systematics calculator SMock [152] for examples. Several analysis techniques avoid this pitfall by fitting for dust and intrinsic color globally, without assuming a prior, though this requires high quality data over several wavelength bands.

6. Future prospects

The main uncertainty in our future ability to map the cosmological expansion is the level of control of systematics we can achieve. In a reductio ad absurdum we can say that since one supernova explodes every second in the universe we might measure 10^7 per year, giving distance accuracies of $10\%/\sqrt{10^7} = 0.003\%$ in ten redshift slices over a ten year survey; or counting every acoustic mode in the universe per redshift slice spanning the acoustic scale λ determines the power spectrum to $\lambda^3/(H^{-2}\lambda) = (1/30)^2$ or 0.1%; or measuring weak lensing shear across the full sky with 0.1” resolution takes individual 1% shears to the 0.0003% level. Statistics is not the issue: understanding of systematics is.

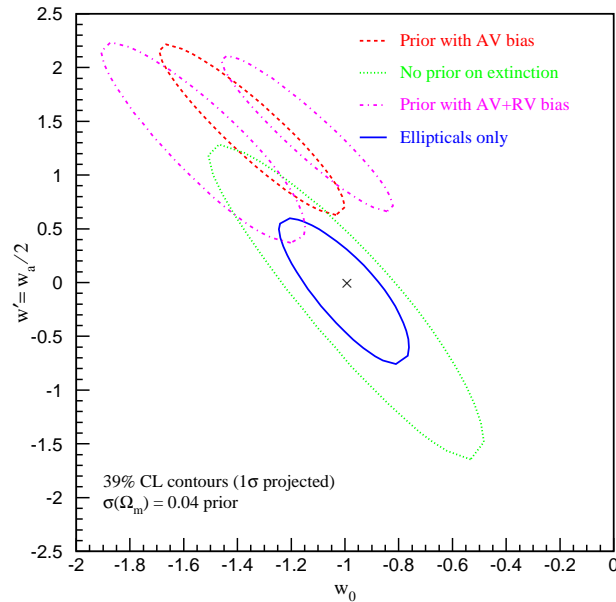


Figure 18. Assuming a prior on dust properties (A_V and R_V) in order to reduce extinction errors can cause systematic deviations in the magnitudes. These give strong biases to the equation of state, leading to a false impression of a transition from $w < -1$ to $w > -1$. To avoid this systematic, one can use samples with minimal extinction (elliptical galaxy hosted supernovae) or obtain precise multiwavelength data that allows for fitting the dust and color properties. Based on [153].

6.1. Data and systematics

However it is much easier to predict the future of statistical measurements than systematic uncertainties. It is difficult to estimate what the future prospects really are. Large surveys are being planned assuming that uncertainties will be solved – or if the data cannot be used for accurately mapping the cosmic expansion it will still prove a cornucopia to many fields of astrophysics. Moreover, an abundance of surveys mentioned in the literature are various levels of vaporware: many have never passed a national peer review or been awarded substantial development funding or had their costs reliably determined. Rather than our listing such possibilities, the reader can peruse national panel reports such as the ESA Cosmic Vision program [154], US National Academy of Sciences’ Beyond Einstein Program Assessment Committee report [155], or the upcoming US Decadal Survey of Astronomy and Astrophysics [156].

The current situation regarding treatment of systematics is mixed. In supernova cosmology, rigorous identification and analysis of systematics and their effects on parameter estimation is (almost) standard procedure. In weak lensing there exists the Shear Testing Programme [157], producing and analyzing community data challenges. Other techniques have less organized systematics analysis, where it exists, and the crucial rigorous comparison of independent data sets (as in [43]) is rare. Control methods such

as blind analysis are also rare. We cannot yet say where the reality will lie between the unbridled statistical optimism alluded to in the opening of this section and current, quite modest measurements. Future prospects may be bright but considerable effort is still required to realize them.

6.2. Mapping resolution

Since prediction of systematics control is difficult, let us turn instead to intrinsic limits on our ability to map the expansion history – limits that are innate to cosmological observables. The expansion history $a(t)$, like distances, is an integral over $H = d \ln a / dt$, and does not respond instantaneously to the evolution of energy density (which in turn is an integral over the equation of state). As seen in Figures 7-8, the cosmological kernel for the observables is broad – no fine toothed comb exists for studying the expansion. This holds even where models have rapid time variation $w' > 1$, as in the e-fold transition model, or when considering principal components (see [158, 129] for illustrations).

(This resolution limit on mapping the expansion is not unique to distances – the growth factor is also an integral measure and the broad kernel of techniques like weak lensing is well known. The Hubble parameter determined through BAO, say, requires a redshift shell thickness $\Delta z \gtrsim 0.2$ to obtain sufficient wave modes for good precision, limiting the mapping resolution.)

Thus, due to the innate cosmological dependences of observables, plus additional effects such as Nyquist and statistics limits of wavemodes in a redshift interval and coherence of systematics over redshift [158], we cannot expect mapping of the cosmological expansion with finer resolution than $\Delta z \approx 0.2$ from next generation data.

6.3. Limits on cosmic doomsday

Finally, we turn from the expansion history to the expansion future. As pointed out in §2.5, to determine the fate of our universe we must not only map the past expansion but understand the nature of the acceleration before we can know the universe's destiny – eternal acceleration, fading of dark energy, or recollapse.

We do not yet have that understanding, but suppose we assume that the linear potential model of dark energy [38], perhaps the simplest alternative to a cosmological constant, is correct. Then we can estimate the time remaining before the fate of recollapse: the limit on cosmic doomsday. The linear potential model effectively has a single equation of state parameter and is well approximated by the family with $w_a = -1.5(1 + w_0)$ when w_0 is not too far from -1 . Curves of the expansion history (and future) are illustrated in the left panel of Figure 19; the doomsday time from the present is given by

$$t_{\text{doom}} \approx 0.5 H_0^{-1} (1 + w_0)^{-0.8}. \quad (24)$$

The current best constraints from data (cf. [159] for future limits) appear in the right panel of Figure 19, corresponding to $t_{\text{doom}} > 24$ Gy at 68% confidence level. It is

obviously of interest to us to know whether the universe will collapse and how long until it does, so accurate determination of w_a is important! The difference between doomsday in only two Hubble times from now and in three (a whole extra Hubble time!) is only a difference of 0.12 in w_a .

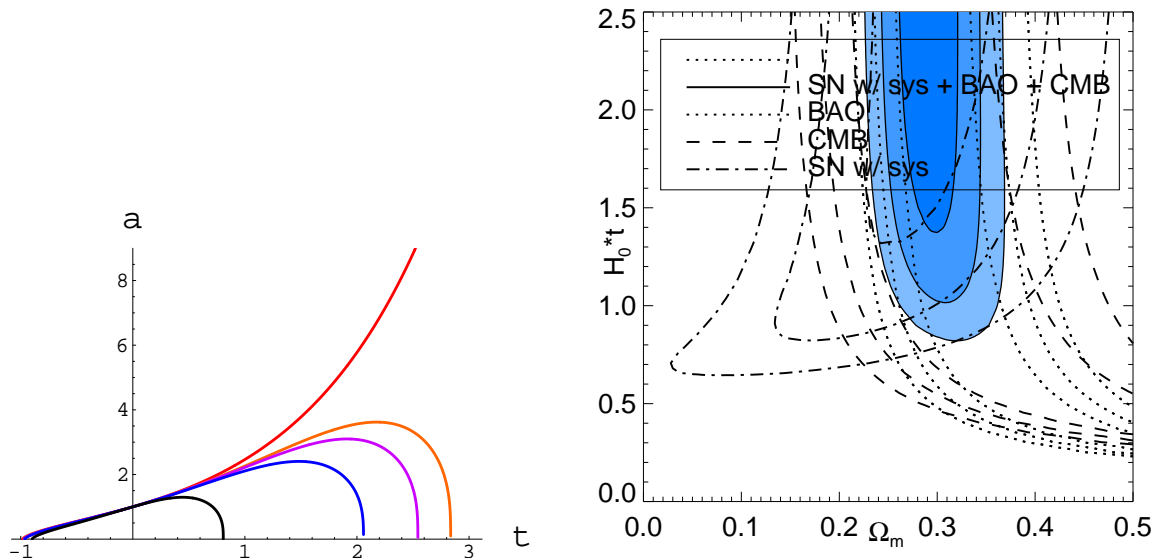


Figure 19. The future expansion history in the linear potential model has a recollapse, or cosmic doomsday. *Left panel:* Precision measurements of the past history are required to distinguish the future fate, with the five curves corresponding to five values for the potential slope (the uppermost curve is for a flat potential, i.e. a cosmological constant). From [159]. *Right panel:* Current data constraints estimate cosmic doomsday will occur no sooner than ~ 1.5 Hubble times from now. From [160].

7. Conclusions

Mapping the cosmological expansion is a key endeavour in our quest for understanding physics – gravitation and other forces, spacetime, the vacuum – and the origin, evolution, and future of the universe. The Big Bang model of a hot, dense, early universe expanding and adiabatically cooling, and forming structure through gravitational instability from primordial seed perturbations, is remarkably successful and simple. The concordance cosmology is (close to) spatially flat and 13.7 billion years old. This clear statement represents a substantial advance of our knowledge over a decade ago.

The discovery of the acceleration of the cosmic expansion created a renaissance of cosmological exploration, offering the hope of connecting quantum physics and gravitation, extra dimensions and the nature of spacetime, while severing the bonds between geometry and destiny. This opens up completely two premier questions in science: the origin and the fate of the universe. To understand the nature of the gravitationally repulsive dark energy pulling the universe apart, we must map the cosmological expansion in greater detail and accuracy than ever envisioned.

We have shown that a considerable part of the optimal approach for mapping the expansion history is set purely by the innate cosmological dependences. Observational programs must follow these foundations as basic science requirements: in particular the need for a wide range of redshifts, $z \approx 0 - 2$ and robust anchoring to either low or high redshift. Our capabilities for measuring the expansion through direct geometric probes are increasing, and techniques are continuing to develop. There are no short cuts – detailed design of successful surveys works within this framework with the purpose to minimize systematic uncertainties in the measurements.

Every technique has systematic uncertainties, appearing in multiple guises. While observational systematics are most familiar, arising even in purely geometric techniques, equally important are issues in the data analysis, e.g. combining heterogeneous data sets, and in the theoretical interpretation, e.g. susceptibility to biases from assumptions of high redshift behavior or of non-expansion physics (perturbation growth behavior, coupling, etc.).

We have given several concrete examples of the effects of systematic uncertainties for various probes. These provide a cautionary tale for survey design, as we are now entered into the systematics dominated data era – and may well soon approach the theory systematics era. We cannot rely on assumptions that any part of the dark sector is simple and ignorable while we concentrate on another aspect. For true progress, we emphasized the role of complementarity in building from robust, clean answers to more complex investigations. Probes employing growth of structure give windows on both expansion per se and gravitational laws, and we commented that the excitement of testing general relativity is equally matched with the challenge of creating a framework for analysis.

Acceleration of the cosmic expansion heralds a revolution in physics, if we can characterize and understand it. To comprehend this new aspect of the universe, we must map the expansion not only at recent epochs, but encompass the early universe. Once we have garnered sufficient understanding, the prize is answering the question of the fate of the universe, now unbound from the question of the cosmic geometry. The good news is that we likely have at least 24 billion years to do so!

Acknowledgments

I thank the Aspen Center for Physics for a superb working environment, and Los Alamos National Laboratory and the Santa Fe 07 workshop, University of Heidelberg, and the Dark Cosmology Centre and Niels Bohr Summer Institute, for hospitality. I gratefully acknowledge contributions by Georg Robbers, Ramon Miquel, and David Rubin of Figures 11, 18, and 19 respectively. Colleagues too numerous to mention helped form my thinking on this wide ranging topic, but I will single out Bob Wagoner for laying the foundations. This work has been supported in part by the Director, Office of Science, Department of Energy under grant DE-AC02-05CH11231.

References

- [1] Focus issue on dark energy 2008, Gen. Rel. Grav. 40, xx-xx
- [2] Bernstein J & Feinberg G (eds) 1986, *Cosmological Constants: Papers in Modern Cosmology* (Columbia U Press: New York)
- [3] Riess A G et al. 1998, Astron. J. 116, 1009-1038
- [4] Perlmutter S et al. 1999, ApJ 517, 565-586
- [5] Frieman J A, Turner M S, Huterer D 2008, Ann. Rev. Astron. Astroph. 46, in press
- [6] Sandage A 1962, ApJ 136, 319-333
- [7] McVittie G 1962, ApJ 136, 334-338
- [8] Linder E V 1991, at <http://supernova.lbl.gov/~evlinder/drift.html>
- [9] Linder E V 1997, *First Principles of Cosmology* (London: Addison-Wesley)
- [10] Uzan J-P, Bernardeau F, Mellier Y 2007, arXiv:0711.1950
- [11] Blandford R D, Amin M, Baltz E A, Mandel K, Marshall P J 2005, ASP Conf. Ser. 339, 27-38
[arXiv:astro-ph/0408279]
- [12] Rapetti D, Allen S W, Amin M A, Blandford R D 2007, MNRAS 375, 1510-1520
- [13] Shapiro C & Turner M S 2006, ApJ 649, 563-569
- [14] Weinberg S 1989, Rev. Mod. Phys. 61, 1-23
- [15] Carroll S M 2001, Liv. Rev. Rel. 4, 1
- [16] Bousso R 2008, Gen. Rel. Grav. 40, xxx
- [17] Caldwell R R & Linder E V 2005, Phys. Rev. Lett. 95, 141301
- [18] Linder E V 2008, Gen. Rel. Grav. 40, xxx
- [19] Olive K A & Peacock J A 2007, at <http://pdg.lbl.gov/2007/reviews/bigbangrpp.pdf>
- [20] Lahav O & Liddle A R 2007, at <http://pdg.lbl.gov/2007/reviews/hubblerrpp.pdf>
- [21] Sachs R K 1961, Proc. Roy. Soc. London A 264, 309-338
- [22] Kristian J & Sachs R K 1966, ApJ 143, 379-399
- [23] Gunn J E 1967, ApJ 150, 737-753
- [24] Jacobs M W, Linder E V, Wagoner R V 1992, Phys. Rev. D 45, R3292-R3295
- [25] Stoeger W R, Araujo M E, Gebbie T 1997, ApJ 476, 435-439 ; erratum ApJ 522, 559
- [26] Feynman R P 1964, unpublished lecture notes
- [27] Zel'dovich Y B 1964, Sov. Ast. 8, 13-16
- [28] Dyer C C & Roeder R C 1972, ApJ 174, L115-L117
- [29] Linder E V 1998, arXiv:astro-ph/9801122
- [30] Ishibashi A & Wald R M 2006, Class. Quant. Grav. 23, 235-250
- [31] Linder E V 1988, Astron. Astroph. 206, 190-198
- [32] Lineweaver C H & Davis T M 2005, Sci. Am. 292, 36-45
- [33] Krauss L M & Starkman G D 2000, ApJ 531, 22-30
- [34] Krauss L M & Scherrer R J 2007, Gen. Rel. Grav. 39, 1545-1550
- [35] Rindler W 2006, *Relativity: Special, General, and Cosmological* (Oxford: Oxford U. Press)
- [36] Caldwell R R, Kamionkowski M, Weinberg N N 2003, Phys. Rev. Lett. 91, 071301
- [37] Linder E V 2004, Phys. Rev. D 70, 023511
- [38] Linde A 1987, in *Three Hundred Years of Gravitation*, ed. S W Hawking & W Israel (Cambridge: Cambridge U. Press), p. 604-630
- [39] Steinhardt P J & Turok N 2002, Science 296, 1436-1439
- [40] Linder E V 2003, Phys. Rev. Lett. 90, 091301
- [41] Kim A G 2008, in *Dark Energy*, ed. P Ruiz-Lapuente (Cambridge: Cambridge U. Press), in press
- [42] Nugent P et al. 2006, ApJ 645, 841-850
- [43] Kowalski M et al. 2008, ApJ submitted
- [44] Efsthathiou G & Bond J R 1999, MNRAS 304, 75-97
- [45] Wright E L 2007, ApJ 664, 633-639
- [46] Frieman J A, Huterer D, Linder E V, Turner M S 2003, Phys. Rev. D 67, 083505

- [47] Hu W, Huterer D, Smith K M 2006, ApJ 650, L13-L16
- [48] Eisenstein D J et al. 2005, ApJ 633, 560-574
- [49] Hütsi G 2006, Astron. Astroph. 449, 891-902
- [50] Padmanabhan, N et al. 2007, MNRAS 378, 852-872
- [51] Cole S et al. 2005, MNRAS 362, 505-534
- [52] Percival W J et al. 2007, MNRAS 381, 1053-1066
- [53] Sanchez A G & Cole S 2007, arXiv:0708.1517
- [54] Padmanabhan N 2008, in preparation
- [55] Meiksin A, White M, Peacock J A 1999, MNRAS 304, 851-864
- [56] Cooray A 2002, in *A New Era in Cosmology*, ASP Conf. Proc. 283, 162-163
[arXiv:astro-ph/0112418]
- [57] Eisenstein D 2002, ASP Conf. Proc. 280, 35-42
- [58] Blake C & Glazebrook K 2003, ApJ 594, 665-673
- [59] Linder E V 2003, Phys. Rev. D 68, 083504
- [60] Hu W & Haiman Z 2003, Phys. Rev. D 68, 063004
- [61] Seo H-J & Eisenstein D J 2003, ApJ 598, 720-740
- [62] Glazebrook K & Blake C 2005, ApJ 631, 1-20
- [63] White M 2005, Astropart. Phys. 24, 334-344
- [64] Linder E V 2005, arXiv:astro-ph/0507308
- [65] Seo H-J & Eisenstein D J 2005, ApJ 633, 575-588
- [66] Battistelli E S et al. 2002, ApJ 580, L101-L104
- [67] Tolman R C 1930, Proc. Nat. Acad. Sci. 16, 511-520
- [68] Ruse H S 1932, Proc. Roy. Soc. Edinburgh 52, 183-194
- [69] Etherington I M H 1933, Phil. Mag. 15, 761
- [70] Weinberg S 1972, *Gravitation and Cosmology* (Wiley: New York)
- [71] Ellis G F R 1971, in *General Relativity and Cosmology*, ed. R Sachs (London: Academic Press),
p. 104-182
- [72] Carroll S M & Kaplinghat M 2002, Phys. Rev. D 65, 063507
- [73] Zahn O & Zaldarriaga M 2003, Phys. Rev. D 67, 063002
- [74] Chan K C & Chu M-C 2007, Phys. Rev. D 75, 083521
- [75] Chung, D J H, Everett L L, Kong K, Konstantin T 2007, JHEP 10, 016
- [76] Griest K 2002, Phys. Rev. D 66, 123501
- [77] Friedman A S & Bloom J S 2005, ApJ 627, 1-25
- [78] Butler N R, Kocevski D, Bloom J S, Curtis J L 2007, ApJ 671, 656-677
- [79] Schutz B F 1986, Nature 323, 310-311
- [80] Holz D E & Hughes S A 2005, ApJ 629, 15-22
- [81] Jain B & Taylor A 2003, Phys. Rev. Lett. 91, 141302
- [82] Bernstein G & Jain B 2004, ApJ 600, 17-25
- [83] Zhang J, Hui L, Stebbins A 2005, ApJ 635, 806-820
- [84] Jimenez R, Verde L, Treu T, Stern D 2003, ApJ 593, 622-629
- [85] Simon J, Verde L, Jimenez R 2005, Phys. Rev. D 71, 123001
- [86] Verkhodanov O V, Parijskij Y N, Starobinsky A A 2005, Bull. SAO 58, 5-15 [arXiv:0705.2776]
- [87] Daly R et al. 2007, arXiv:0710.5112
- [88] Kaspi S 2007, ASP Conf. Ser. 373, 13-22 [arXiv:0705.1722]
- [89] Teerikorpi P 2005, arXiv:astro-ph/0510382
- [90] Siegel E R et al. 2005, MNRAS 356, 1117-1122
- [91] Fry J N 1985, Phys. Lett. B 158, 211-214
- [92] Linder E V 1988, MPA internal research note
- [93] Linder E V 2006, Astropart. Phys. 26, 16-21
- [94] Mészáros P 1974, Astron. Astroph. 37, 225-228
- [95] Bernardeau F, Colombi S, Gaztañaga E, Scoccimarro R 2002, Phys. Rep. 367, 1-248

- [96] Tegmark M et al. 2006, Phys. Rev. D 74, 123507
- [97] Mcdonald P et al. 2006, ApJS 163, 80-109
- [98] Gunn, J E & Tinsley, B M 1975, Nature 257, 454-457
- [99] Loh, E D & Spillar E J 1986, ApJ 307, L1-L4
- [100] Jarvis M, Jain B, Bernstein G, Dolney D 2006, ApJ 644, 71-79
- [101] Benjamin J et al. 2007, MNRAS 381, 702-712
- [102] Semboloni E et al. 2006, Astron. Astroph. 452, 51-61
- [103] Massey R et al. 2007, ApJS 172, 239-253
- [104] Fu L et al. 2007, arXiv:0712.0884
- [105] Doré et al. 2007, arXiv:0712.1599
- [106] Hu W, Holz D E, Vale C 2007, Phys. Rev. D 76, 127301
- [107] Lue A, Scoccimarro R, Starkman G 2004, Phys. Rev. D 69, 124015
- [108] Knox L, Song Y-S, Tyson J A 2006, Phys. Rev. D 74, 023512
- [109] Ishak M, Upadhye A, Spergel D 2006, Phys. Rev. D 74, 043513
- [110] Linder E V 2005, Phys. Rev. D 72, 043529
- [111] Huterer D & Linder E V 2007, Phys. Rev. D 75, 023519
- [112] Linder E V & Cahn R N 2007, Astropart. Phys. 28, 481-488
- [113] Caldwell R, Cooray A, Melchiorri A 2007, Phys. Rev. D 76, 023507
- [114] Zhang P, Liguori M, Bean R, Dodelson S 2007, Phys. Rev. Lett. 99, 141302
- [115] Amendola L, Kunz M, Sapone D 2007, arXiv:0704.2421
- [116] Hu W & Sawicki I 2007, Phys. Rev. D 76, 104043
- [117] Amin M, Wagoner R, Blandford R 2007, arXiv:0708.1793
- [118] Jain B & Zhang P 2007, arXiv:0709.2375
- [119] Dvali G, Gabadadze G, Porrati M 2000, Phys. Lett. B 485, 208-214
- [120] Keeton C R & Petters A O 2006, Phys. Rev. D 73, 104032
- [121] Uzan, J-P 2003, Rev. Mod. Phys. 75, 403-455
- [122] Kunz M & Sapone D 2007, Phys. Rev. Lett. 98, 121301
- [123] Song Y-S, Sawicki I, Hu W 2007, Phys. Rev. D 75, 064003
- [124] DeDeo S, Caldwell R R, Steinhardt P J 2003, Phys. Rev. D 67, 103509
- [125] Amendola L 2004, Phys. Rev. D 69, 103524
- [126] Mangano G, Melchiorri A, Serra P, Cooray A, Kamionkowski M 2006, Phys. Rev. D 74, 043517
- [127] Linder E V 2003, at <http://supernova.lbl.gov/~evlinder/gdotsn.pdf>
- [128] Huterer D & Starkman G 2003, Phys. Rev. Lett. 90, 031301
- [129] de Putter R & Linder E V 2007, arXiv:0710.0373
- [130] Linder E V & Huterer D 2005, Phys. Rev. D 72, 043509
- [131] Linder E V 2007, arXiv:0708.0024
- [132] Frieman J A, Hill C T, Stebbins A, Waga I 1995, Phys. Rev. Lett. 75, 2077-2080
- [133] Crittenden R, Majerotto E, Piazza F 2007, Phys. Rev. Lett. 98, 251301
- [134] Doran M & Robbers G 2006, JCAP 0606, 026
- [135] Doran M, Robbers G, Wetterich C 2007, Phys. Rev. D 75, 023003
- [136] Dvali G & Turner M S 2003, arXiv:astro-ph/0301510
- [137] Jönsson J, Goobar A, Amanullah R, Bergström L 2004, JCAP 0409, 007
- [138] Tegmark M 2002, Phys. Rev. D 66, 103507
- [139] Linder E V 2004, Phys. Rev. D 70, 061302
- [140] Francis M J, Lewis G F, Linder E V 2007, MNRAS 380, 1079-1086
- [141] Linder E V 2006, Astropart. Phys. 26, 102-110
- [142] Doran M, Stern S, Thommes E 2007, JCAP 0704, 015
- [143] Linder E V & Robbers G, in draft
- [144] Eisenstein D J & White M 2004, Phys. Rev. D 70, 103523
- [145] Branch D, Perlmutter S, Baron E, Nugent P 2001, arXiv:astro-ph/0109070
- [146] Hui L & Greene P B 2006, Phys. Rev. D 73, 123526

- [147] Cooray A & Caldwell R R 2006, Phys. Rev. D 73, 103002
- [148] Neill J D, Hudson M J, Conley A 2007, ApJ 661, L123-L126
- [149] Cooray A, Huterer D, Holz D E 2007, Phys. Rev. Lett. 96, 021301
- [150] LoVerde M, Hui L, Gaztañaga E 2007, arXiv:0708.0031
- [151] Upadhye A, Ishak M, Steinhardt P J 2005, Phys. Rev. D 72, 063501
- [152] Nordin J, Goobar A, Jönsson J 2008, JCAP in press [arXiv:0801.2484] ;
further information and calculator at <http://www.physto.se/~nordin/smock>
- [153] Linder E V & Miquel R 2004, Phys. Rev. D 70, 123516
- [154] Cosmic Vision 2007, at <http://sci.esa.int/science-e/www/area/index.cfm?fareaid=100>
- [155] BEPAC 2007, at http://books.nap.edu/catalog.php?record_id=12006
- [156] Astro2010 Survey, at <http://www7.nationalacademies.org/bpa/Astro2010.html>, in preparation
- [157] Shear Testing Programme, at http://www.physics.ubc.ca/~heymans/step/cosmic_shear_test.html
Heymans C et al. 2006, MNRAS 368, 1323-1339 ;
Massey R et al. 2007, MNRAS 376, 13-38
- [158] Linder E V 2007, Phys. Rev. D 75, 063502
- [159] Kallosh R, Kratochvil J, Linde A, Linder E V, Shmakova M 2003, JCAP 0310, 015
- [160] Rubin D, Kowalski M, Linder E V, Perlmutter S 2008, in draft